Final Report for NAG-1-02090

Metals Technology for Aerospace Applications in 2020: Development of High Temperature Aluminum Alloys For Aerospace Applications

Prepared by:
Professor Edgar A. Starke, Jr.
Department of Materials Science and Engineering
University of Virginia
116 Engineer's Way
Charlottesville, VA 22904

Prepared for:
National Aeronautics and Space Administration
Office of Management Scientific and Technical Information Programs

For Review by:
Mr. Dennis Dicus
Grant Monitor
Metallic Materials Branch
Langley Research Center
Hampton, Virginia 23665

October 15, 2003

Executive Summary

The ultimate goal of this research program is to raise the viable service temperature for the next generation of Al-Cu-Mg-Ag-X alloys to about 150°C. The major objectives of this work are to optimize the precipitation hardening for balanced mechanical properties and to enhance the thermal stability of the selected strengthening phases. We selected the Ω plate-like precipitates with habit plane {111} and the θ' plate-like precipitates with habit plane {100} as strengthening phases for this system. We do not want our alloy to contain the S phase, which is normally present in most commercial Al-Cu-Mg alloys, since it has an adverse effect on the thermal stability of the Ω phase. A fine uniform dispersion of the co-existing θ' and Ω plates in certain combinations is desired.

This Langley Research Center Grant under NAG-1-02090 supported Mr. Brian M. Gable, who is pursuing a Doctor of Philosophy degree in Materials Science and Engineering at the University of Virginia. During the one year period of this Grant Mr. Gable completed a significant amount of research, which resulted in the following publications that are attached as the body of this final report:

1. B.M. Gable, G.J. Shiflet and E.A. Starke, Jr., "The Effect of Si Additions on the Nucleation of Ω in Al-Cu-Mg Alloys," presented at TherMec '03, Madrid, Spain, and published in Materials Science Forum, Vols. 426-432 (2003) pp. 471-476.

2. B.M. Gable, G.J. Shiflet and E.A. Starke, Jr., "The Effect of Si Additions on the Nucleation of Ω in Al-Cu-Mg Alloys," Scripta Materialia, in press.

3. Aiwu Zhu, Brian M. Gable, Gary J. Shiflet, Edgar A. Starke, Jr., "Elastic Strain Energy Analysis of Trace-Element Clusters in Al-Cu-Mg-X Alloys: A First Principle Total Energy Calculation," First International Symposium on Metallurgical Modeling for Aluminum Alloys, Pittsburg, PA, October, 2003, in press.

4. Aiwu Zhu, Brian M. Gable, Gary J. Shiflet, Edgar A. Starke, Jr., "Formation of Clusters for Precipitation in Al-Cu-Mg-(Ag, Si) Alloys: Short-Range-Ordering and Strain-Energy Analysis," The Third International Conference on Light Materials for Transportation Systems, Honolulu, Hawaii, November, 2003, in press.

The Effect of Si Additions on the Nucleation of Ω in Al-Cu-Mg Alloys

B.M. Gable, G.J. Shiflet & E.A. Starke, Jr.
Light Metals Center, Materials Science & Engineering Department
116 Engineer's Way, P.O. Box 400745
University of Virginia, Charlottesville, VA, USA 22904-4745
bmg6g@virginia.edu, gjs@virginia.edu, eas1o@virginia.edu

Keywords: Al-Cu-Mg alloys, Si additions, Ω, σ, θ', S-phase, competitive precipitation

Abstract. The role of trace additions on the nucleation and stability of the primary strengthening phase, Ω, is of paramount importance for the enhancement of mechanical properties for moderate temperature application of Al-Cu-Mg-(Ag) alloys. In order to better understand the competition for solute, which governs the microstructural evolution of these alloys, a series of Al-Cu-Mg-Si quaternary alloys were prepared to investigate the role of trace Si additions on the nucleation of the Ω phase. Si additions were found to quell Ω nucleation in conjunction with the enhanced matrix precipitation of competing phases. These initial results indicate that it is necessary to overcome a critical Mg/Si ratio for Ω precipitation, rather than a particular Si content.

Introduction & Background

Al-Cu-Mg-Ag alloys are currently under development as potential precipitation hardened materials for moderate-temperature and high-strength applications in the aerospace industry because of their excellent thermal stability [1-3]. Current efforts to further enhance the creep resistance and strength at elevated temperatures of these alloys have focused on maintaining a fine and thermally stable distribution of the Ω phase. This has placed emphasis on obtaining a better understanding of the role of trace additions and their effects on the microstructural evolution and stability of Ω in Al-Cu-Mg ternary and higher order systems.

Ω Precipitation. The Ω phase, believed to be a variant of equilibrium Al_2Cu (θ), is most commonly found in high purity Al-Cu-Mg-Ag-X alloys, forming uniformly on the $\{111\}_\alpha$ matrix planes with Mg and Ag segregated to the coherent interphase boundaries with the α matrix [2-4]. Vaughn and Silcock reported a $\{111\}_\alpha$ θ variant in a binary Al-4.0Cu ($^{wt}/_o$) alloy aged at temperatures in excess of 350°C [5]. There is no other mention in the literature of the presence of a $\{111\}_\alpha$ θ variant for the Al-Cu binary system. Little is known about the presence and stability of the Ω in the Al-Cu-Mg ternary system. The Ω phase was first observed in an Al-4.0Cu-0.5Mg ($^{wt}/_o$) ternary alloy aged at 190-250°C by Garg *et al.* in 1990 [6]. The role of Mg in the microstructural evolution of Ω is not well understood, but it is believed to be a critical component for nucleation due to the lack of Ω formation in Al-Cu-Ag ternary alloys and in Al-Cu binary alloys aged at moderate temperatures. More recently several groups have observed Ω precipitation in Al-Cu-Mg-X alloys without the presence of Ag [7-12]. The authors reported enhanced Ω precipitation through high temperature aging [7], the introduction of dislocations from cold working [10], the addition of Cd [9] and substantial natural aging prior to artificial aging [12].

Competitive Precipitation. Artificial aging of traditional Al-Cu-Mg ternary alloys at moderate temperatures may result in the precipitation of several phases Al_2Cu (θ'), Al_2Cu (θ), Al_2Cu (Ω), Al_2CuMg (S) and $Al_5Cu_6Mg_2$ (σ) [13,14]. It is important to note that each of these phases is in competition for nucleation sites and solute.

A factor which has been shown to hinder matrix Ω precipitation and stability in Al-Cu-Mg-(Ag) alloys is the presence of Si [15-18]. This effect may be attributed to the high binding energy between Si and Mg and that trace additions of Si have also been shown to stimulate matrix precipitation of θ', S and σ phases, which are competing for solute [18-23]. It is important to note that despite the rigorous studies performed on a wide variety of Al-Cu-Mg alloys from 1906-1960's the Ω phase, in the absence of Ag, was not identified until 1990 [6]. Revisiting a summary of the studies performed on Al-Cu-Mg alloys from 1929-1954 (summarized in [24]) one can see that the Si content of the majority of the alloys studied exceeded $0.1^{wt}/_{o}$. Many of these alloys intentionally implemented Si additions to increase strength and hardness (arising from enhanced matrix precipitation of the strengthening phases). These Si levels may have led to the suppression of Ω precipitation in these early Al-Cu-Mg alloys, which was not observed until microstructural characterization was performed on high purity alloys.

Early work on Al-Cu-Mg alloys by Polmear [25] and Vietz and Polmear [26] focused on the role of trace additions of Ag and Si on subsequent mechanical properties. Their work showed that additions of either Ag *or* Si increased the age hardening response of Al-Cu-Mg alloys, while the trace addition of Si to Al-Cu-Mg-Ag alloys only led to nominal gains in hardness. Similarly, the addition of Ag to alloy L65, Al-4.3Cu-0.8Mg-0.7Si-0.8Mn (with a Mg/Si ratio of ~1.1) had little effect on age hardening [25].

Recent differential scanning calorimetry (DSC) and transmission electron microscopy (TEM) work by Abis, *et al.* demonstrated that the addition of 0.15-0.50Si ($^{wt}/_{o}$) to an Al-4.5Cu-0.3Mg-0.7Ag-0.25Ti ($^{wt}/_{o}$) alloy eliminated Ω precipitation when aged at 190°C [15,16]. The authors state that Si suppressed Ω′ nucleation (their proposed precursor to Ω), which prevented subsequent Ω precipitation. Abis, *et al.* reported enhancement in θ′ and S matrix precipitation associated with Si additions. A similar study conducted by Y.S. Lee, *et al.* [17] demonstrated that the addition of 0.1Si and 0.1Ge to an Al-5.5Cu-0.3Mg-0.4Ag alloy ($^{wt}/_{o}$) suppressed Ω precipitation, in turn driving θ′ and S matrix precipitation when artificially aged at moderate temperatures. The authors noted that the enhanced age hardening response associated with the trace addition of Ag was quelled by the presence of Si and Ge due to the exhaustion of the available Mg [17]. There was no mention of σ phase precipitation in either study.

Several recent studies by Wang, *et al.* [27] and Mukhopadhyay, *et al.* [28,29] have focused on Ω precipitation in various 2024-type alloys containing appreciable Si levels. In their work Wang and Mukhopadhyay observed Ω precipitation in alloys with Si levels as high as $0.50^{wt}/_{o}$ and $0.65^{wt}/_{o}$, respectively. The Ω nucleation primarily occurred heterogeneously on Mn-containing dispersoids. This work may indicate that the deleterious nature of Si may be related to the alloy Mg/Si ratio, rather than a critical Si content considering equivalent Si additions completely eliminated Ω precipitation in low Mg-containing alloys. A summary of pertinent investigations into the evolution of the Ω phase may be found in Table I. It is important to note that the smaller the Mg/Si ratio the more likely that Ω precipitation was eliminated. Further consideration concerning the study by Lee, *et al.* must also take into account the Mg-binding effects from the presence of Ge [30,31].

The objective of this study is to investigate the role of trace Si additions on the nucleation of the Ω phase in Al-4.0Cu-xMg alloys. Due to the fact that the next generation of Al-Cu-Mg-Ag alloys for moderate temperature application may require low Mg levels, in order to suppress S-phase formation for optimal Ω precipitation, it is paramount to assess the possible deleterious nature of trace Si levels that ultimately dictate the subsequent microstructural evolution.

Table I – Summary of Ω Precipitation in Al-Cu-Mg-Si-X alloys

Alloy Composition [$^{wt}/_{o}$]	Reference	Mg/Si ratio	Ω Precipitation
Al-4.4Cu-0.3Mg-0.7Ag-0.3Mn-0.2Ti-0.50Si	[15,16]	0.6	no
Al-4.4Cu-0.3Mg-0.7Ag-0.3Mn-0.2Ti-0.28Si	[15,16]	1.1	no
Al-4.5Cu-0.3Mg-0.7Ag-0.3Mn-0.2Ti-0.15Si	[15,16]	2.0	no
Al-5.0Cu-1.45Mg-0.70Mn-0.40Ag-0.65Si-0.13Fe	[29]	2.2	yes
Al-5.5Cu-0.3Mg-0.4Ag-0.1Si-0.1Ge	[17]	3.0	no
Al-4.4Cu-1.5Mg-0.6Mn-0.5Si-0.5Fe	[27]	3.0	yes
Al-4.4Cu-1.5Mg-0.6Mn-0.2Si-0.3Fe	[27]	7.5	yes
Al-4.5Cu-0.3Mg-0.7Ag-0.3Mn-0.2Ti-0.03Si	[15,16]	10.0	yes
Al-3.3Cu-0.76Mg-0.56Ag-0.07Si-0.08Fe	[18]	10.9	yes
Al-5.0Cu-0.54Mg-0.029Si-0.038Fe	[10]	18.6	yes
Al-4.0Cu-0.47Mg-0.005Si-0.006Fe	[6]	94.0	yes

Experimental Procedure

Alloy Preparation. The various Al-Cu-Mg-X alloys used throughout this study were produced in our laboratories using high purity metals, precisely weighed for each desired alloy composition, resulting in a 5g charge. Once weighed, the Si lump, Al and Cu shot were arc-melted together into "buttons" under an Ar atmosphere. The Mg additions were not arc-melted along with the other elements due to its high vapor pressure and low boiling point. The arc-melted button was then weighed to discern any possible weight loss, presumably from the evaporation of Al under the intense arc, and subsequently sand blasted to remove the exterior surface. The button and raw Mg (wrapped in high purity Al foil) were then induction cast together in a graphite crucible coated with a thin layer of BN paste. Good mixing of the raw materials was ensured during both the arc-melting and induction-melting procedures.

After induction-melting each ingot was again sandblasted to remove the exterior surface and rolled (~10% reduction) in order to introduce deformation to expedite the subsequent homogenization procedure. Once rolled, the ingot was sectioned and encapsulated in Pyrex tubing back-filled with Ar. The encapsulated alloys were then placed in a tube furnace at room temperature and heated to temperatures ~510°C, remaining at this temperature for 72h. After the water quench from the homogenization temperature each ingot was sectioned, rolled, solution heat treated at 530°C for 1h, water quenched and immediately artificially aged at 250°C for 2h in a circulating air box furnace. A ~0.5g portion of each homogenized ingot was independently analyzed for precise final chemistry [32]. The alloy compositions used in this study are listed in Table II.

Transmission Electron Microscopy. Once aged, specimens for transmission electron microscopy (TEM) were ground to an approximate thickness of approximately 150μm, mechanically punched into 3mm discs and electropolished in a 7:2 methanol-nitric acid solution cooled to –23°C in a twin-jet electropolishing unit. The microstructural characterization of the specimens was performed using a 200kV TEM.

Table II – Al-Cu-Mg-Si quaternary alloy compositions used in this study

Nominal Alloy Composition	Cu [$^{wt}/_{o}$]	Mg [$^{wt}/_{o}$]	Si [$^{wt}/_{o}$]	Fe [ppm]	Al
Al-4.0Cu-0.4Mg high purity	3.87	0.40	<0.005	<50	balance
Al-4.0Cu-0.4Mg-0.1Si	4.09	0.38	0.10	160	balance
Al-4.0Cu-0.4Mg-0.2Si	4.08	0.42	0.22	170	balance
Al-4.0Cu-0.4Mg-0.4Si	4.18	0.40	0.43	170	balance
Al-4.0Cu-0.1Mg-0.1Si	3.83	0.09	0.09	110	balance
Al-4.0Cu-0.2Mg-0.1Si	3.82	0.18	0.09	86	balance
Al-4.0Cu-0.3Mg-0.1Si	3.90	0.24	0.11	110	balance

Results & Discussion

Table III summarizes the microstructural characterization of the various quaternary Al-Cu-Mg-Si alloys. The data demonstrate that Ω precipitation was suppressed in the alloys with either Mg contents <0.3 $^{wt}/_{o}$ or Si levels ≥ 0.2 $^{wt}/_{o}$. These levels of trace elements correspond to Mg/Si ratios of ≤ 2.0 for the elimination of the Ω phase, which is in agreement with the studies summarized in Table I.

Table III – Summary of TEM Microstructural Characterization of Samples Aged at 250°C for 2h

Al-4.0Cu-Mg-Si [$^{wt}/_{o}$]	Mg	Mg/Si ratio	Ω Precipitation
Constant Si content ~0.1 [$^{wt}/_{o}$]	0.1	1	no
	0.2	2	no
	0.3	3	yes
	0.4	4	yes
Al-4.0Cu-Mg-Si [$^{wt}/_{o}$]	Si	Mg/Si ratio	Ω Precipitation
Constant Mg content ~0.4 [$^{wt}/_{o}$]	<50ppm	80	yes
	0.1	4	yes
	0.2	2	no
	0.4	1	no

Representative TEM micrographs and diffraction patterns of several of the alloys are presented in Figure 1. The artificially aged high purity Al-4.0Cu-0.4Mg alloy contained θ' and Ω plates along with S rods. The addition of 0.1Si ($^{wt}/_{o}$) enhanced the matrix precipitation of θ' plates, stimulated the precipitation of σ cubes and lowered the Ω population. This effect may be seen in the corresponding bright field micrographs and selected area diffraction (SAD) patterns. The streaking and diffraction spots associated with Ω precipitation in the SAD patterns are evident for the high purity alloy, while they are either very faint or absent with the addition of 0.1Si ($^{wt}/_{o}$). The alloy containing 0.2Si ($^{wt}/_{o}$) demonstrated a dense population of σ cubes, with no evidence of Ω precipitation. These initial results support the premise that Ω precipitation was not observed in the early Al-Cu-Mg ternary alloys due to nominal alloy Si content.

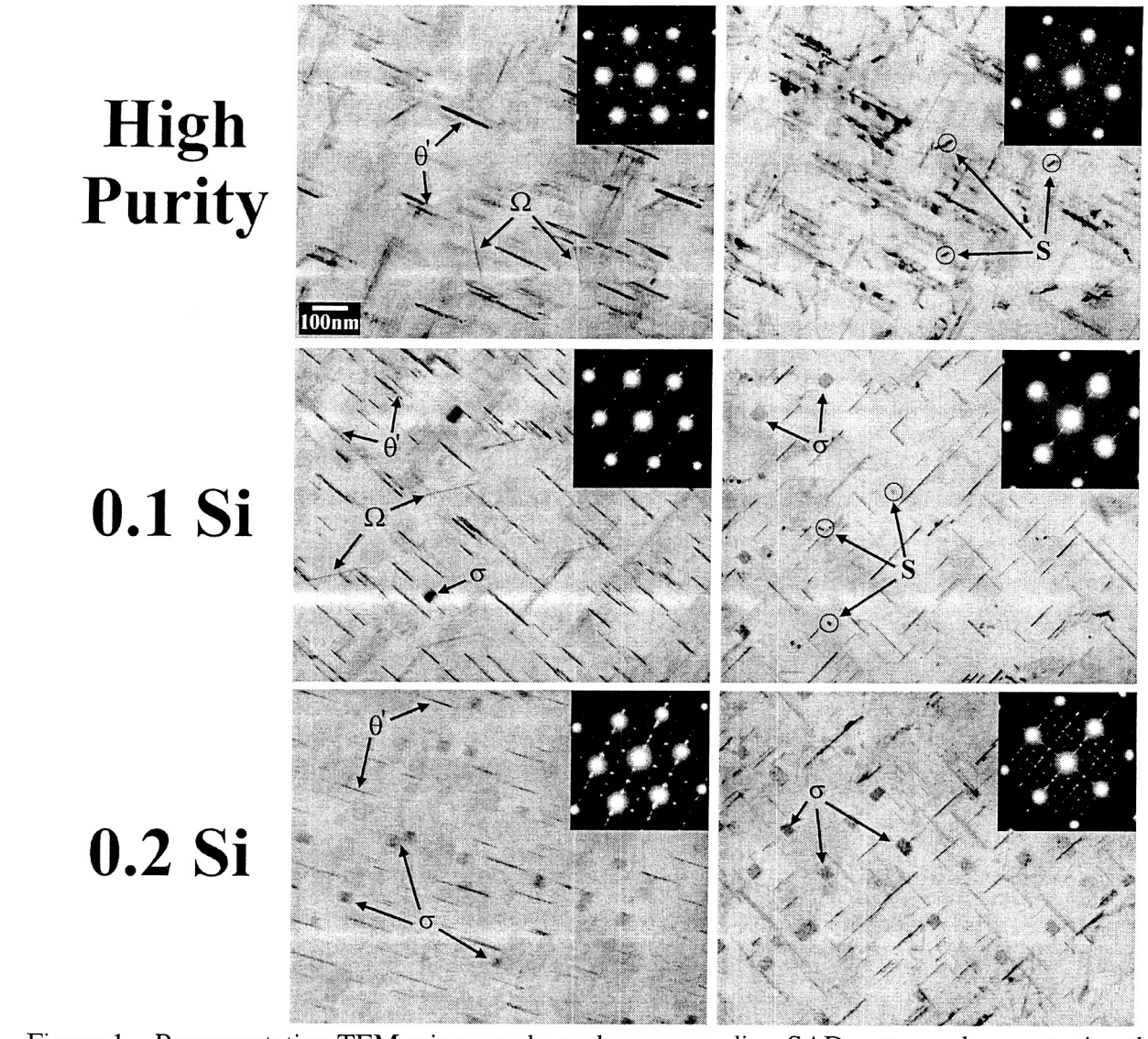

Figure 1 – Representative TEM micrographs and corresponding SAD patterns demonstrating the matrix precipitation in the various Al-4.0Cu-0.4Mg-xSi alloys after artificial aging at 250°C for 2h.

There are several possible explanations for the potent effect of Si content on diminishing Ω precipitation. First, the high binding energy between Si and Mg atoms may have effectively limited the Mg available for subsequent precipitation of those phases dependent upon Mg for nucleation and growth, such as Ω. If the presence of Si disrupts the pre-precipitate Mg-rich clusters, which act as the nucleation aid for Ω precipitation, the subsequent Ω population will suffer.

Another possible effect of Si additions is to alter the competitive precipitation between phases, an effect that is already well documented [19-23]. The enhancement of θ', S and/or σ precipitation will have the direct effect of limiting possible formation of Ω through the consumption of solute. The presence of Si may also alter the competitive precipitation between phases through shifting respective metastable and equilibrium phase boundaries, possibly leading to the instability of Ω plates. The paucity of data identifying Ω crystal structure and phase-space in Al-Cu-Mg-(Ag) alloys limits further discussion on this matter.

Conclusions

This study has demonstrated the effect of Si on quelling Ω precipitation in low Mg-containing alloys. The initial results indicate that in the low-Mg containing alloys a Mg/Si ratio of ~2 must be

overcome in order for Ω nucleation. This sensitivity of Ω precipitation to Si content may explain the absence of Ω precipitation in the early Al-Cu-Mg alloys and must be considered when designing the next generation of Al-Cu-Mg-(Ag) alloys.

Acknowledgements

The authors would like to acknowledge the financial support of the Air Force Office of Scientific Research under Grant No. S49620-01-1-0090, Dr. Craig S. Hartley, Program Manager and the financial support from NASA under Grant NAG-1-02090.

References

[1] I.J. Polmear, G. Pons, Y. Barbaux, H. Octor, C. Sanchez, A.J. Morton, W.E. Borbidge and S. Rogers, Mat. Sci. and Tech., 1999, **15**, 861.
[2] S.P. Ringer, W. Yeung, B.C. Muddle and I.J. Polmear, Acta Metall., 1994, **42**, 5, 1715.
[3] C.R. Hutchinson, X. Fan, S.J. Pennycook and G.J. Shiflet, *ibid.*, 2001, **49**, 2827.
[4] L. Reich, M. Murayama and K. Hono, *ibid.*, 1998, **46**, 17, 6053.
[5] D. Vaughn and J.M. Silcock, Physica Status Solidi, 1967, **20**, 725.
[6] A. Garg, Y.C. Chang and J.M. Howe, Scripta Met., 1990, **24**, 677.
[7] R.W. Fonda, W.A. Cassada and G.J. Shiflet, Acta Metall. Mater., 1992, **40**, 10, 2539.
[8] B.M. Gable, A.W. Zhu, G.J. Shiflet and E.A. Starke, Jr., Materials Design Approaches and Experiences (USA), eds. J.-C. Zhao, M. Fahrmann and T.M. Pollock, 2001, 111.
[9] B.T. Sofyan, I.J. Polmear and S.P. Ringer, Materials Science Forum, 2002, **396-402**, 613.
[10] N. Unlu, B.M. Gable, G.J. Shiflet and E.A. Starke, Jr, *ibid.*, 801.
[11] N. Gao, L. Davin, S. Wang, A. Cerezo and M.J. Starink, *ibid.*, 923.
[12] G.B. Winkelman, K. Raviprasad and B.C. Muddle, *ibid.*, 1037.
[13] S.L. Chen, Y. Zuo, H. Liang and Y.A. Chang, Met. Mat. Trans. A, 1997, **28A**, 435.
[14] T. Jantzen, S.G. Fries, M.G. Harmelin and F. Faudot, Proc. CALPHAD XXVIII, Grenoble, 1999.
[15] S. Abis, P. Mengucci and G. Riontino, ICAA-3, *Al Alloys – Their Physical and Mechanical Properties*, eds. L. Arnberg, O. Lohne, E. Nes and N. Ryum,1992, 231.
[16] S. Abis, P. Mengucci and G. Riontino, Phil. Mag. A, 1994, **70**, 5, 851.
[17] Y.S. Lee, S.P. Ringer, B.C. Muddle and I.J. Polmear, ICAA-4 *Al Alloys – Their Physical and Mechanical Properties*, eds. T.H. Sanders, Jr. and E.A. Starke, Jr., 1994, 582.
[18] Q. Li, Ph.D. Dissertation, University of Virginia, 1995.
[19] R.N. Wilson, D.M. Moore and P.J.E. Forsyth, J. Inst. Metals, 1967, **95**, pp.177-183.
[20] D. Mitlin, V. Radmilovic, J.W. Morris, Jr., Met. and Mat. Trans. A, 2000, **31A**, pp.2697-2711.
[21] H. Suzuki, I. Araki, M. Kanno and K Itoi, Trans. Jpn. Inst. Light Met., 1977, **27**, 239.
[22] R.D. Schueller, A.K. Sachdev and F.E. Wawner, Scripta Met. Mat., 1992, **27**, 617.
[23] J.C. Barlow, W.M. Rainforth and H. Jones, J. Mat. Sci., 2000, **35**, 6, 1413.
[24] H.K. Hardy, J. Inst. Metals, 1954-55, **83**, pp.17-34.
[25] I.J. Polmear, Trans. Met. Soc. A.I.M.E., 1964, **230**, 1331.
[26] J.T. Vietz and I.J. Polmear, J. Inst. Metals, 1966, **94**, 410.
[27] L.M. Wang, H.M. Flower and T.C. Lindley, Scripta Mat., 1999, **41**, 4, 391.
[28] A.K. Mukhopadhyay, G. Eggeler and B. Skrotzki, *ibid.*, 2001, **44**, 545.
[29] A.K. Mukhopadhyay, Met. Mat. Trans. A., 2002, **33A**, 3635.
[30] G.B. Brook and H.B. Hatt, The Mechanism of Phase Transformations in Crystalline Solids, Institute of Metals, London, 1969, 82.
[31] S.P. Ringer, S.P. Swenser, B.C. Muddle, I.J. Polmear and T. Sakurai, Materials Science Forum, 1996, **217-222**, 689.
[32] Wah Chang Analytical Services, Albany, OR, USA 97321, www.wahchang.com.

The Effect of Si Additions on Ω Precipitation in Al-Cu-Mg-(Ag) Alloys

B.M. Gable, G.J. Shiflet & E.A. Starke, Jr.†
Materials Science & Engineering Department
University of Virginia
116 Engineer's Way, Charlottesville, VA, USA 22904-4745
† - corresponding author

Keywords: aluminum alloys; phase transformations; precipitation; trace Si additions; transmission electron microscopy (TEM)

Abstract

A series of Al-Cu-Mg-(Ag)-Si alloys were prepared to investigate the role of Si additions on Ω formation. Trace amounts of Si were found to quell Ω precipitation, indicating that it is necessary to overcome a critical Mg/Si ratio for Ω nucleation in this alloy system, regardless of the presence of Ag.

Introduction & Background

Al-Cu-Mg-Ag alloys are currently under development as potential precipitation hardened materials for moderate-temperature and high-strength applications in the aerospace industry because of their excellent thermal stability [1-3]. Efforts to further enhance the creep resistance and strength at elevated temperatures of these alloys have focused on maintaining a fine and thermally stable distribution of the primary strengthening phase, designated Ω. The Ω phase, believed to be a variant of equilibrium Al_2Cu (θ), is a thin plate-like precipitate with a $\{111\}_\alpha$ habit plane, most commonly found in high purity Al-Cu-Mg-Ag-X alloys. Nucleation of Ω has been shown to occur on Mg-rich clusters aligned along $\{111\}_\alpha$ [4]. The Ω phase was first observed in an Al-4.0Cu-0.5Mg[1] ternary alloy aged at 190-250°C by Garg *et al.* in 1990 [5]. The role of Mg in the microstructural evolution of Ω is not well understood, but it is believed to be a critical component for nucleation because of the lack of Ω formation in Al-Cu-Ag ternary alloys. This has driven recent investigations to determine the role of the trace element additions on Ω precipitation and stability in Al-Cu-Mg ternary and higher order systems.

The addition of Si [6-8] has been shown to hinder the matrix Ω precipitation and stability in Al-Cu-Mg-(Ag) alloys. This effect may be attributed to the high binding energy between Si and Mg. Trace additions of Si have also been shown to stimulate matrix precipitation of Al_2Cu (θ′), Al_2CuMg (S) and $Al_5Cu_6Mg_2$ (σ), which are phases competing for solute [8-13]. Despite the

rigorous studies performed on a wide variety of Al-Cu-Mg alloys from 1906-1960's, the Ω phase, in the absence of Ag, was not identified until 1990 [5]. Revisiting a summary of the studies performed on Al-Cu-Mg alloys from 1929-1954 (summarized in [14]) confirms that the Si content of the majority of the alloys studied exceeded 0.1. Many of these alloys intentionally implemented Si additions to increase strength, which arose from enhanced matrix precipitation of the strengthening phases. As a result, these Si levels may have led to the suppression of Ω precipitation in early Al-Cu-Mg alloys, and Ω was not observed until microstructural characterization was performed on high purity alloys.

Early work on Al-Cu-Mg-X alloys by Polmear [15] and Vietz and Polmear [16] focused on the role of Ag and Si trace additions on subsequent mechanical properties. Their work showed that additions of either Ag *or* Si significantly increased the age hardening response of Al-Cu-Mg alloys, arising from Ω phase precipitation and the refinement of the microstructure, respectively. However, trace Si additions to Al-Cu-Mg-Ag alloys only resulted in nominal gains in hardness. Similarly, the addition of Ag to alloy L65, Al-4.3Cu-0.8Mg-0.7Si-0.8Mn with a Mg/Si ratio of ~1.1, had little effect on age hardening [15].

Recent differential scanning calorimetry (DSC) and transmission electron microscopy (TEM) work by Abis, *et al.* [6] demonstrated that the addition of 0.15-0.50Si to an Al-4.5Cu-0.3Mg-0.7Ag-0.25Ti alloy eliminated Ω precipitation when aged at 190°C. The authors stated that Si suppressed Ω′ nucleation (their proposed precursor to Ω), which prevented subsequent Ω precipitation, and reported an enhancement in θ′ and S matrix precipitation associated with Si additions. A similar study conducted by Lee, *et al.* [7] showed that the addition of 0.1Si and 0.1Ge to an Al-5.5Cu-0.3Mg-0.4Ag alloy suppressed Ω precipitation, in turn driving θ′ and S matrix precipitation when artificially aged at moderate temperatures. The authors noted that the enhanced age hardening response associated with the trace addition of Ag was quelled by the presence of Si and Ge because of the exhaustion of the available Mg [7]. There was no mention of σ phase precipitation in either study.

The most complete microstructural and hardness characterization study to date on the effects of trace Si additions to Al-Cu-Mg-(Ag) alloys was conducted by Gao, *et al.* [8] on a series of Al-4.0Cu-0.3Mg-(0.4Ag) alloys with Si levels ranging between 0-0.7Si. The addition of 0.1Si greatly reduced the measured hardness of the base Al-4.0Cu-0.3Mg-0.4Ag alloy, which corresponded to an inhibition of Ω precipitation. Further additions of Si enhanced the hardness of the alloy, but

[1] The alloy compositions throughout this manuscript will be given in terms of $^{wt}/_{o}$, unless stated otherwise.

eliminated the formation of Ω plates. The authors [8] only observed Ω precipitation in Ag-containing alloys with less than 0.2Si.

A summary of pertinent investigations into the evolution of the Ω phase is listed in Table I. It is important to note that the smaller the Mg/Si ratio the more likely that Ω precipitation was eliminated. Further consideration of the study by Lee, *et al.* [7] must also take into account the Mg-binding effects from the presence of Ge [18,19].

The objective of this study was to investigate the role of trace Si additions on the formation of the Ω phase in Al-Cu-Mg-(Ag) alloys. Because the next generation of Al-Cu-Mg-Ag alloys for moderate temperature application may require low Mg levels, in order to suppress S-phase formation for optimal Ω stability, it is necessary to assess the possible deleterious nature of trace Si levels on the subsequent microstructural evolution.

Experimental Procedure

The Al-Cu-Mg-(Ag)-(Si) alloys used throughout this study were produced in our laboratories using 99.999% Al shot, 99.9% Cu shot, 99.99% Mg pellets, 99.9985% Ag wire and 99.995% Si lump (metals basis) purity elements, resulting in a 5g charge. Once weighed, the Si, Ag (if necessary), Al and Cu were arc-melted together into "buttons" under an Ar atmosphere. The Mg additions were not arc-melted along with the other elements because of its high vapor pressure and low boiling point. The arc-melted button and pure Mg (wrapped in high purity Al foil) were then induction cast together in a graphite crucible coated with a thin layer of boron nitride paste. Good mixing of the raw materials was ensured during both the arc-melting and induction-melting procedures.

After induction-melting each ingot was cold-rolled (~20% reduction) to expedite the subsequent homogenization, sectioned, encapsulated in glass tubing back-filled with Ar and homogenized at ~510°C for 72h. After the water quench from the homogenization temperature each ingot was sand-blasted, rolled to a final thickness of ~0.85mm, solution heat treated at 525°C for 1h, water quenched and immediately artificially aged at 250°C for either 30min or 2h in a circulating air box furnace. Previous work [5,17] has shown that aging at 250°C leads to a higher volume fraction of Ω versus aging at a lower temperature, *e.g.* 150°C-200°C, with the early aging times allowing for investigation into the nucleation of the competing phases.

A ~0.5g portion of each homogenized ingot was independently analyzed for precise final chemistry [20]. The alloy compositions used in this study are listed in Table II. The Mg/Si ratios

used throughout this study are in terms of $^{wt}/_{o}$, but should be approximately the same in terms of $^{at}/_{o}$ considering the similarity between their atomic weights, 24.3g/mole and 28.1g/mole, respectively.

Once aged, specimens for TEM were ground to a thickness of approximately 150μm, mechanically punched into 3mm discs and electropolished in a 7:2 methanol-nitric acid solution cooled to –23°C in a twin-jet unit. The microstructural characterization of the specimens was performed using a 200kV TEM.

Results & Discussion

Representative TEM micrographs and corresponding $<110>_{\alpha}$ selected area diffraction (SAD) patterns are presented in Figure 1 for the Al-4.0Cu-0.4Mg-xSi alloys and Figure 2 for those alloys with an additional 0.3Ag. The bright field images were taken near the $<110>_{\alpha}$ zone axis. The artificially aged high purity Al-4.0Cu-0.4Mg and Al-4.0Cu-0.4Mg-0.3Ag alloys contained θ′ and Ω plates along with S laths, with Ω precipitation dominating in the Ag-containing alloy. The addition of 0.1Si enhanced the matrix precipitation of θ′ plates, stimulated the precipitation of σ cubes and lowered the number density of Ω plates for both alloys, regardless of artificial aging time or Ag content. This effect can be seen in the corresponding bright field micrographs and SAD patterns. The streaking along $\{111\}_{\alpha}$ and the diffraction spots at $^{1}/_{3}$ and $^{2}/_{3}$ $[220]_{\alpha}$ associated with Ω precipitation in the SAD patterns are evident for the high purity alloys, while they are either very faint or absent for those alloys with 0.1Si. The alloys containing 0.2Si possessed a high density of θ′ plates and σ cubes, with no evidence of Ω precipitation. The finely spaced diffraction spots associated with σ precipitation [12,13] are visible in the SAD patterns for the Si-containing alloys. A comparison of Figures 1 and 2 demonstrates that when the Mg/Si ratio is ~2.0, the presence of Ag has no effect on the subsequent microstructure. It is important to note that there is no significant difference in the type of precipitation observed between the 30min and 2h aging conditions.

Table III summarizes the presence of Ω plates in the Al-4.0Cu-xMg-(0.3Ag)-xSi alloys aged at 250°C. The data demonstrate that Ω precipitation was suppressed in the alloys with Mg/Si ratios of ≤ 2.0, regardless of Mg and Si content. This indicates that Ω precipitation is not dictated by a critical Si content, but rather by the Mg/Si ratio of the alloy. These results are in good agreement with the studies summarized in Table I.

There are several possible explanations for the potent effect of Si content on diminishing Ω precipitation. First, the high binding energy between Si and Mg atoms may effectively limit the Mg available for the formation of pre-precipitate Mg-rich clusters along $\{111\}_{\alpha}$, which act as a nucleation aid for Ω precipitation. Presumably the Mg-Si attraction is greater than that associated

with Mg-Ag pairs based upon the elimination of Ω precipitation. If the presence of Si disrupts the evolution of these Mg-rich clusters the subsequent Ω density will be diminished. The effect of Si influencing the creation of Mg-rich clusters is supported by work of Pabi [21] and Hutchinson and Ringer [22]. The resistivity work by Pabi [21] demonstrated that Si affected the solute zone formation in a series of Al-Cu-Mg-Si alloys, which lead to the proposition of Si incorporation in solute clusters. Hutchinson and Ringer [22] later used energy dispersive spectroscopy (EDS) to demonstrate that Si was in fact present in the GPB zones formed at 200°C.

Another possible effect of Si additions is to alter the competitive precipitation between phases, an effect that is already well documented [8-13]. The enhancement of θ′, S and/or σ precipitation will have the direct effect of limiting possible formation of Ω through the depletion of solute. The presence of Si may also alter the competitive precipitation between phases through shifting metastable and equilibrium phase boundaries, possibly leading to the instability of Ω plates. The paucity of data identifying the Ω crystal structure and phase-space in Al-Cu-Mg-(Ag) alloys limits further discussion on this matter.

Also, it must be considered whether Ω precipitation in alloys with very low Mg concentrations, *e.g.* <0.3, is even possible. Early work by Chester and Polmear [23] reported minor Ω precipitation in an Al-4.0Cu-0.1Mg-0.4Ag alloy, stating that θ′ was the primary phase after artificial aging at 200°C. This supports the notion that Mg-rich clusters act as the heterogeneous nucleation sites for Ω plates since the matrix precipitation of a similar 0.3Mg alloy was dominated by the Ω phase [2,3,23]. Previous atom probe work by Reich, *et al.* [4] demonstrated that the Mg/Ag atomic ratio in the Mg-Ag clusters was approximately 1.0. When considering this class of Al-Cu-Mg-Ag alloys, the Ag concentration is typically on the order of $0.4^{wt}/_{o}$ ($\sim 0.1^{at}/_{o}$). If the Mg-Ag clusters do possess a Mg/Ag atomic ratio of 1.0, then Ω precipitation in an alloy with a Mg concentration on the order of $0.1^{wt}/_{o}$ ($\sim 0.1^{at}/_{o}$) should be sufficient for the same number density of Ω plates. However, according to the results from this study, these extremely low Mg concentrations would only require 500ppm of Si to exhaust the Mg, eliminating Ω precipitation. The Si content of most commercial "high purity" alloys is on the order of 100-300ppm.

Conclusions

This study has demonstrated that trace amounts of Si, depending on the Mg content, were responsible for limiting Ω precipitation in both Al-Cu-Mg and Al-Cu-Mg-Ag base alloys. The results indicate that a Mg/Si ratio of ~2.0 must be overcome for Ω nucleation. This sensitivity of Ω

precipitation to the alloy Mg/Si ratio may explain the absence of Ω in the early Al-Cu-Mg alloys and should be taken into consideration when designing the next generation of Al-Cu-Mg-(Ag) alloys.

Acknowledgements

The authors would like to acknowledge the financial support of the Air Force Office of Scientific Research under Grant No. S49620-01-1-0090, Dr. Craig S. Hartley, Program Manager and the financial support from NASA under Grant NAG-1-02090.

References

[1] I.J. Polmear, G. Pons, Y. Barbaux, H. Octor, C. Sanchez, A.J. Morton, W.E. Borbidge and S. Rogers. Mat. Sci. and Tech. 1999;15:861.
[2] S.P. Ringer, W. Yeung, B.C. Muddle and I.J. Polmear. Acta Metall. 1994;42:1715.
[3] C.R. Hutchinson, X. Fan, S.J. Pennycook and G.J. Shiflet. Acta Metall. 2001;49:2827.
[4] L. Reich, M. Murayama and K. Hono. Acta Metall. 1998;46:6053.
[5] A. Garg, Y.C. Chang and J.M. Howe. Scripta Mat. 1990;24:677.
[6] S. Abis, P. Mengucci and G. Riontino. Phil. Mag. A 1994;70:851.
[7] Y.S. Lee, S.P. Ringer, B.C. Muddle and I.J. Polmear. ICAA-4 Proc., eds. T.H. Sanders, Jr. and E.A. Starke, Jr. 1994;582.
[8] X. Gao, J.F. Nie and B.C. Muddle, Mat. Sci. Forum 1996;217-222:1251.
[9] R.N. Wilson, D.M. Moore and P.J.E. Forsyth. J. Inst. Metals 1967;95:177.
[10] D. Mitlin, V. Radmilovic, J.W. Morris, Jr. Met. and Mat. Trans. A 2000;31A:2697.
[11] H. Suzuki, I. Araki, M. Kanno and K Itoi. Trans. Jpn. Inst. Light Met. 1977;27:239.
[12] R.D. Schueller, A.K. Sachdev and F.E. Wawner. Scripta Met. Mat. 1992;27:617.
[13] J.C. Barlow, W.M. Rainforth and H. Jones. J. Mat. Sci. 2000;35:1413.
[14] H.K. Hardy. J. Inst. Metals 1954-55;83:17.
[15] I.J. Polmear. Trans. Met. Soc. A.I.M.E. 1964;230:1331.
[16] J.T. Vietz and I.J. Polmear. J. Inst. Metals 1966;94:410.
[17] N. Unlu, B.M. Gable, G.J. Shiflet and E.A. Starke, Jr. Met.Trans.A; in press.
[18] G.B. Brook and H.B. Hatt. The Mechanism of Phase Transformations in Crystalline Solids. London: Inst. of Metals; 1969:82.
[19] S.P. Ringer, S.P. Swenser, B.C. Muddle, I.J. Polmear and T. Sakurai. Mat. Sci. Forum 1996;217-222:689.
[20] Wah Chang Analytical Services. Albany, OR, USA 97321. www.wahchang.com.
[21] S.K. Pabi. NML Technical Journal 1976;18:10.
[22] C.R. Hutchinson and S.P. Ringer. Met. Mat. Trans. A 2000; 31A:2721.
[23] R.J. Chester and I.J. Polmear. The Metallurgy of Light Metals. London: Inst. of Metals; 1983. p. 75.

Table I – Summary of Ω Precipitation in Al-Cu-Mg-(Ag)-Si-X alloys

Alloy Composition [$^{wt}/_{o}$]	Reference	Mg/Si ratio	Ω Precipitation
Al-4.4Cu-0.3Mg-0.7Ag-0.3Mn-0.2Ti-0.50Si	[6]	0.6	no
Al-4.4Cu-0.3Mg-0.7Ag-0.3Mn-0.2Ti-0.28Si	[6]	1.1	no
Al-4.0Cu-0.3Mg-0.4Ag-0.2Si	[8]	1.5	no
Al-4.5Cu-0.3Mg-0.7Ag-0.3Mn-0.2Ti-0.15Si	[6]	2.0	no
Al-5.5Cu-0.3Mg-0.4Ag-0.1Si-0.1Ge	[7]	3.0	no
Al-4.0Cu-0.3Mg-0.4Ag-0.1Si	[8]	3.0	yes
Al-4.5Cu-0.3Mg-0.7Ag-0.3Mn-0.2Ti-0.03Si	[6]	10.0	yes
Al-5.0Cu-0.54Mg-0.029Si-0.038Fe	[17]	18.6	yes
Al-4.0Cu-0.47Mg-0.005Si-0.006Fe	[5]	94.0	yes

Table II – Al-4.0Cu-xMg-(0.3Ag)-xSi alloy compositions used in this study

Nominal Alloy Composition [$^{wt}/_{o}$]	Cu [$^{wt}/_{o}$]	Mg [$^{wt}/_{o}$]	Ag [$^{wt}/_{o}$]	Si [$^{wt}/_{o}$]	Fe [$^{wt}/_{o}$]	Al
Al-4.0Cu-0.4Mg	3.87	0.40	--	<0.005	<0.005	balance
Al-4.0Cu-0.1Mg-0.1Si	3.83	0.09	--	0.09	0.01	balance
Al-4.0Cu-0.2Mg-0.1Si	3.82	0.18	--	0.09	0.01	balance
Al-4.0Cu-0.3Mg-0.1Si	3.90	0.24	--	0.11	0.01	balance
Al-4.0Cu-0.4Mg-0.1Si	4.09	0.38	--	0.10	0.02	balance
Al-4.0Cu-0.4Mg-0.2Si	4.08	0.42	--	0.22	0.02	balance
Al-4.0Cu-0.6Mg-0.2Si	4.03	0.61	--	0.20	0.02	balance
Al-4.0Cu-0.8Mg-0.2Si	3.99	0.78	--	0.18	0.01	balance
Al-4.0Cu-0.4Mg-03Ag	3.87	0.39	0.28	0.03	0.02	balance
Al-4.0Cu-0.1Mg-0.3Ag-0.1Si	3.95	0.10	0.32	0.06	0.02	balance
Al-4.0Cu-0.2Mg-0.3Ag-0.1Si	4.00	0.20	0.32	0.07	0.02	balance
Al-4.0Cu-0.3Mg-0.3Ag-0.1Si	4.00	0.27	0.32	0.07	0.05	balance
Al-4.0Cu-0.4Mg-0.3Ag-0.1Si	3.94	0.42	0.23	0.11	0.02	balance
Al-4.0Cu-0.4Mg-0.3Ag-0.2Si	4.06	0.46	0.32	0.19	0.02	balance
Al-4.0Cu-0.6Mg-0.3Ag-0.2Si	3.99	0.59	0.26	0.17	0.02	balance
Al-4.0Cu-0.8Mg-0.3Ag-0.2Si	4.20	0.80	0.31	0.21	0.01	balance

Table III – Summary of Ω precipitation for specimens artificially aged at 250°C

Al-4.0Cu-xMg-xSi (■) Al-4.0Cu-xMg-0.3Ag-xSi (◊) [$^{wt}/_{o}$]	Mg [$^{wt}/_{o}$]	Mg / Si ratio [$^{wt}/_{o}$] ~ [$^{at}/_{o}$]	Ω Precipitation		
			no	minor phase	major phase
High Purity <0.03Si	0.4	> 10		■	◊
Constant Si content ~0.1	0.1	1	■ ◊		
	0.2	2	■ ◊		
	0.3	3		■ ◊	
	0.4	4		■ ◊	
Constant Si content ~0.2	0.4	2	■ ◊		
	0.6	3		■ ◊	
	0.8	4		■ ◊	

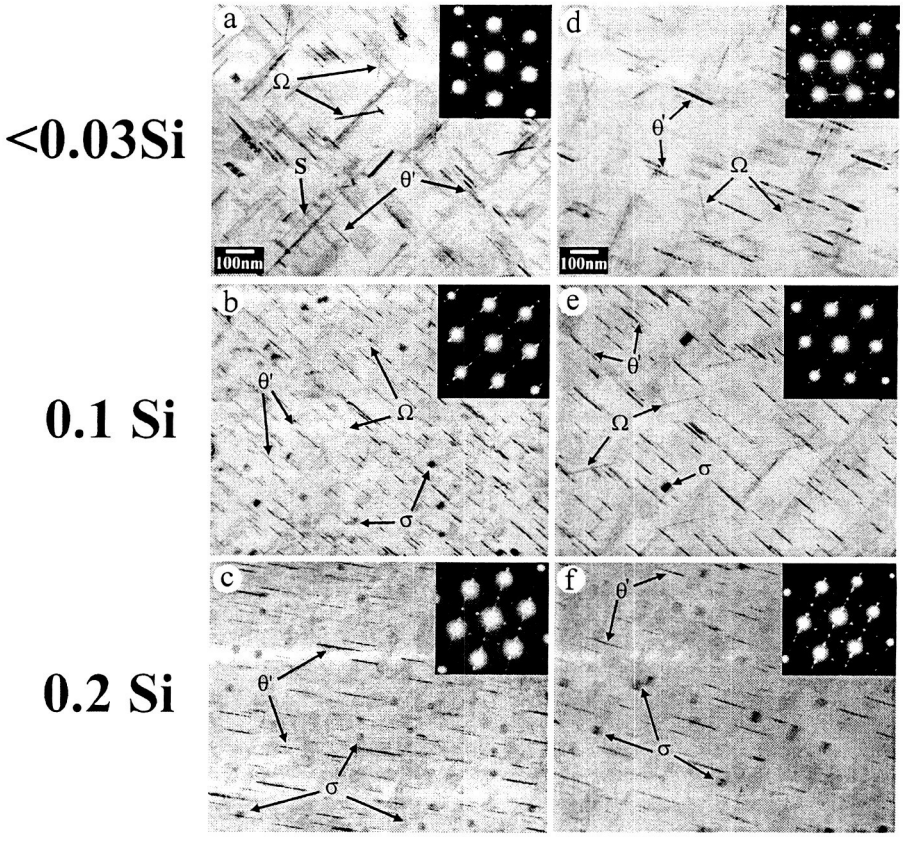

Figure 1 – TEM bright field micrographs and corresponding SAD patterns demonstrating the matrix precipitation in the various Al-4.0Cu-0.4Mg-xSi alloys after artificial aging at 250°C; a-c) aged 30min, d-f) aged 2h.

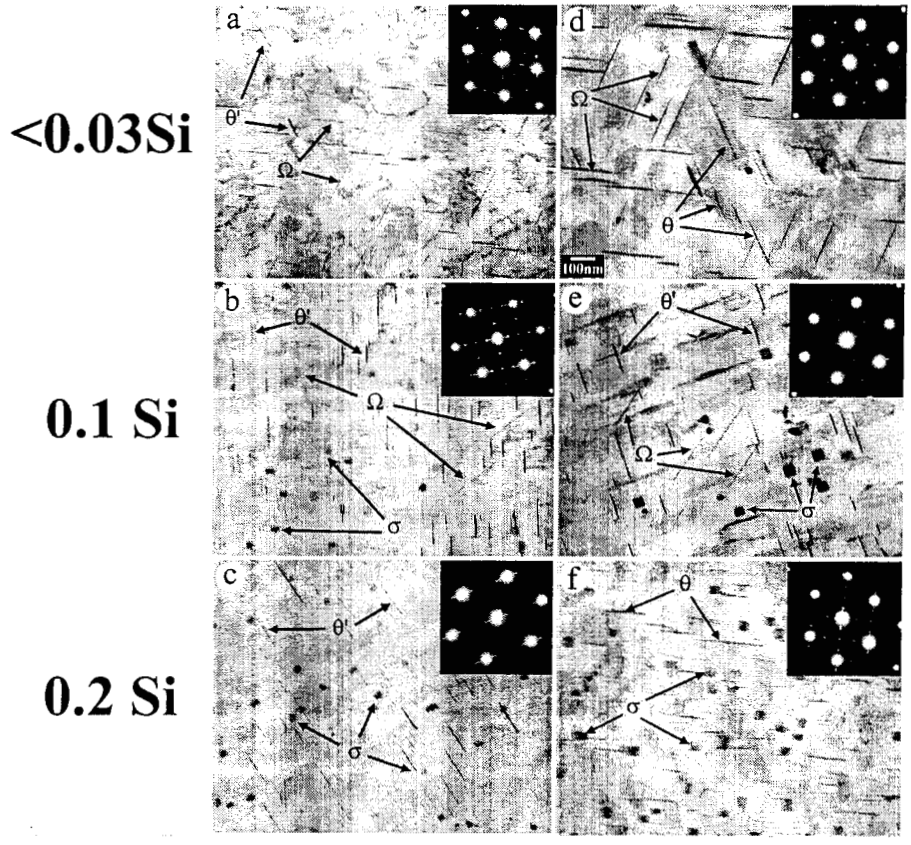

Figure 2 – TEM bright field micrographs and corresponding SAD patterns demonstrating the matrix precipitation in the various Al-4.0Cu-0.4Mg-0.3Ag-xSi alloys after artificial aging at 250°C; a-c) aged 30min, d-f) aged 2h.

Elastic Strain Energy Analysis of Trace-Element Clusters in Al-Cu-Mg-X Alloys: A First Principle Total Energy Calculation

Aiwu Zhu, Brian M Gable, Gary J Shiflet, Edgar A Starke Jr.

Department of Materials Science and Engineering

University of Virginia, 116 Engineer's Way, Charlottesville, VA-22904

Abstract

This paper reports elastic strain energy analysis for the formation of platelet-like pure metal clusters in Al-alloys. The 2nd order elastic tensors are calculated using the first principle total energy. The anisotropy of the strain energy dictates the habit plane selections of the platelet clusters, which are potential precursors for various strengthening precipitates in aluminum-copper based alloys.

Experimental Background

The majority of commercial aluminum alloys are very complex, employing several alloying additions in order to tailor the microstructure and subsequent mechanical properties. Trace alloying additions may contribute to solid solution strengthening, lead to the creation of second phase zones or particles, control grain size and texture, affect corrosion behavior and possibly shift metastable or equilibrium phase boundaries, etc. When considering the formation of second phase particles for strengthening, trace additions may play critical roles in the nucleation, coarsening and stability of the desirable precipitates. The ability to predict and optimize the behavior of trace alloying additions on the microstructural evolution is paramount to the advancement of the next generation of age-hardenable Al-based alloys.

The formation of fine solute clusters and/or zones have been shown to have a great influence on the nucleation of desirable second phase particles in high-strength Al-Cu based alloys. Specifically, Mg, Ag, Zn and Si additions play critical roles in dictating the initial stages of decomposition from the super-saturated solid solution and ultimately control the microstructural evolution between the competing $\{100\}_\alpha$ and $\{111\}_\alpha$ plate-like precipitates, which are the primary strengthening phases for this class of alloys.

Mg Additions

The trace addition of Mg has several marked effects on the vacancy concentration, solute clustering and subsequent microstructural evolution in Al-Cu binary alloys. The presence of Mg may also lead to the creation of other second phase particles, such as Al_2CuMg (S) and a $\{111\}_\alpha$ variant of Al_2Cu, designated Ω. S-phase particles evolve from Cu/Mg-rich solute clusters (GPB zones) that form along $\{100\}_\alpha$ at the initial stages of decomposition. The nucleation of Ω in Al-Cu-Mg ternary alloys is not well understood, but Mg-rich clusters are assumed to play a critical role due to the lack of a $\{111\}_\alpha$ variant of Al_2Cu in binary Al-Cu alloys aged at moderate temperatures. Similarly, trace additions of Mg to Al-Li-Cu alloys have been shown to enhance the matrix nucleation of the equilibrium phase Al_2CuLi (T_1), which is also a plate-like precipitate that forms on $\{111\}_\alpha$ [1].

Mg+Ag Additions

The addition of Ag to Al-Cu-Mg alloys (with approximately 0.3wt% Mg) dramatically enhances the matrix nucleation density of Ω. This beneficial effect arising from Ag additions does not occur when Mg is absent. Recent three-dimensional atom probe work (3D-AP) by Reich, *et al.* [2] revealed that Mg and Ag cluster, with a Mg/Ag atomic ratio of 1.0, along the $\{111\}_\alpha$. These Mg/Ag co-clusters, in turn, act as heterogeneous nucleation sites for the Ω plates, arising from the alleviation of the shear strain barrier associated with the matrix precipitation of these phases [3]. Z-contrast microscopy coupled with high-resolution EDS spectra collection and 3DAP work demonstrated that Mg and Ag were present at the α/Ω and α/T_1 matrix interphase boundaries [2,4-5]. The presence of this Ag-containing segregation was found to correlate with enhanced coarsening resistance of these second phase particles.

Mg+Zn Additions

Recent research by Pickens [6] indicated that Zn additions to an Al-1.0Li-4.0Cu-0.4Mg ($^{wt}/_{o}$) alloy aided T_1 matrix nucleation. Presumably this affect also arises from the

formation of Mg-rich clusters that in turn act as the heterogeneous nucleation sites for matrix T_1 precipitation.

Mg+(Ag)+Si Additions

The addition of Si to these alloys, whether intentional or inherent as a tramp element, dramatically affects the solute clustering behavior. Even in dilute quantities, Si influences Mg-containing cluster formation. Trace additions of Si to Al-Cu-Mg-(Ag) alloys have been found to quell the matrix precipitation of the Ω phase[7-8], which is dependent upon Mg-rich clusters along $\{111\}_\alpha$ to nucleate the plate-like precipitate. In turn, the Si additions stimulate the precipitation of $Al_5Cu_6Mg_2$ (σ) [9] and enhance the matrix nucleation of θ′ and S [10-11], which are phases competing for solute with the Ω phase. Presumably, the Mg-Si clusters or Si-stabilized GPB zones form preferentially the Mg-Ag co-clusters over the Ω phase.

Selection of Trace Elements

The strategy in new aluminum alloy development involves addition of "useful" trace elements and preclusion of "deleterious" impurity elements in order to enhance the formation of precipitates of the desired type, *e.g.*, the Ω phase in Al-Cu based alloys and T1-phases in Al-Li-Cu alloys, leading to the desired fine and uniform dispersion of the strengthening precipitates in the thermo-mechanically treated products.

Generally, the final precipitate structures produced through age hardening processes are greatly controlled by the initial formation of certain elemental clusters or atom aggregates. They act as the precursors to the various, more thermodynamically stable, precipitates. There are two ways to transform the clusters to precipitates. Local strain fields around the clusters due to the lattice misfits provide heterogeneous nucleation sites for precipitates. For platelet-like clusters, since the strain field is highly orientation dependent, they affect the selection of the habit planes of the precipitates. The examples are Mg-rich clusters for the T_1 $\{111\}_\alpha$ in Al-Li-Cu-Mg and Ω $\{111\}_\alpha$ phase in Al-Cu-Mg-(Ag). Secondly, the clusters are often reported to evolve themselves into the precipitates, *e.g.*, the Cu $\{100\}_\alpha$ clusters or [G.P.] zones for θ′ or θ $\{100\}_\alpha$ plates in Al-Cu based alloys. On the other hand, the habit-plane selection of the clusters themselves is controlled by the anisotropy of the lattice-misfit induced strain [12].

Therefore fundamental knowledge is needed for the alloy design about 1) the chemistry of the clusters and 2) the habit plane selection of the platelet-like clusters. While 3D-atom probe and some other analytical microstructure characterization may be employed for experimental investigation, combination of thermodynamic modeling based on the available databases with analysis of the strain or deformation associated with the formation of the clusters may offer some quick information or clues for the element selection and categorization for the alloy design purpose.

As the first step of this research, the strain energy analysis of the pure elemental clusters, using 2nd order elastic constants calculated based on the first principle total energy is reported in the following.

Calculation of Elastic Constants

The formation of the clusters or atom aggregates in the originally homogeneous solid state solutions causes local deformation or distortion of the crystalline lattices due to the lattice misfit between the matrix and the clusters. The deformation may be characterized in the simplest way as "linearly elastic" using the 2nd order elastic tensors. Anisotropy of the elasticity of both crystals hence determines the orientation dependence of the associated strain energy.

While considerable information exists on the elastic moduli of pure metals, the determination of the elastic tensors for the "metastable" *e.g.* magnesium FCC-A1 or "unstable", *e.g.*, silicon–FCC-A1 crystal structures, is impractical. The first principle total energy calculation provides a simple way to the solution. The 2nd order elastic constants of the crystalline solid may be defined and calculated according to the variation in the energy from its optimized lattice structure as

$$C_{ijkl} = \left(\frac{\partial E}{\partial \underline{\varepsilon}_{ij} \partial \underline{\varepsilon}_{kl}}\right)_{E=E_{\min}} \quad i,j,k,l = 1,2, \text{ or } 3 \qquad (1)$$

where E denotes the total energy calculated and $\{\underline{\varepsilon}_{ij}\}$the strain tensor. Using "engineering" notations, Hooke's law may be written: $\sigma_i = \sum_{j=1}^{6} C_{ij}\varepsilon_j$ where $\{\sigma_i\}$ is the stress. By applying strains, or change in the unit cell dimensions, in certain patterns, the variation of the energy or the resulting stress tensor can be then retrieved and the elastic tensors $\{C_{ijkl}\}$ or $\{S_{ijkl}\}$ calculated.

The Vienna *ab-initio* simulation program (VASP) [13] is employed where the density functional theory plane-wave pseudo-potential method is applied. Mainly LDA (Local-Density-Approximation) is used for electronic exchange correlation potentials. GGAs (General-Gradient-approximation), such as PWE and PW91 functionals, are also being tested. The ultrasoft

pseudo-potentials, supplied with the VASP-package, are utilized. The GGA did not produce any significant changes in most of our results. The basis-set cut-offs were set to "high accuracy" and k-point meshes are set by "Monkhorst-Pack" (or Γ-centered) setting from 8×8×8 to 32×32×32 (or otherwise indicated) depending on the size of the unit cell concerned. Table 1 lists the calculated relaxed lattice parameters and the elastic constants for Al, Cu, Ag, Li (fcc-A1) and Mg (hcp-A3). Note that the results, although strictly for 0 K, are quite consistent with the experimental measurements [14]. The elastic tensors for FCC-A1 structures of Mg, Si and Cd are also listed. The negative values of (C11-C12) [15] of the Cd and Si-FCC-A1 structures indicate that the structure is unstable with respect to certain deformations leading to the corresponding symmetry breaking. For comparison, an FCC-A1 structure was constructed using a unit cell of 32 atoms to simulate a "disordered" mixture cluster of composition Cu1-Mg3. The 2nd order elastic constants for this mixture aggregate are also calculated.

Table 1. Elastic constants calculated using VASP and obtained from experiments at room temperature for some element crystals

Element	Structure	Lattice Constants, Å	Elastic Constants, 10^{10} N/m^2	
			Calculated	Experiments
Al	Fcc-A1	4.045	C_{11}=9.30, C_{12}=6.38, C_{44}=3.13	C_{11}=10.8 C_{12}=6.13 C_{44}=2.85
Cu	Fcc-A1	3.642	C_{11}=17.9, C_{12}=12.4, C_{44}=8.03.	C_{11}=16.84,C_{12}=12.14,C_{44}=7.54
Ag	Fcc-A1	4.160	C_{11}=10.93,C_{12}=8.39,C_{44}=3.78	C_{11}=12.4,C_{12}=9.34,C_{44}=4.61
Mg	Hcp-A3	a=3.173, c=5.187	C_{11}=5.39, C_{33}=4.78, C_{12}=2.39, C_{13}=3.26, C_{44}=1.75	C_{11}=5.64, C_{33}=5.81, C_{12}=2.32, C_{13}=1.81, C_{44}=1.68
Mg	Fcc-A1	4.520	C_{11}=4.6, C_{44}=3.0, C_{12}=2.74	n.a.
Li	Fcc-A1	4.286	C_{11}=1.4, C_{12}=1.0, C_{44}=0.7	C11=1.4, C12=1.1, C44=0.9
Cd	Fcc-A1	4.502	C11=3.0, C12=4.9, C44=3.3	n.a.
Si	Fcc-A1	3.894	C11=2.8, C12=10.2, C44=4.2	n.a
CuMg3	FCC-A1	4.219	C_{11}=5.61,C_{12}=2.87, C_{44}=1.12	n.a

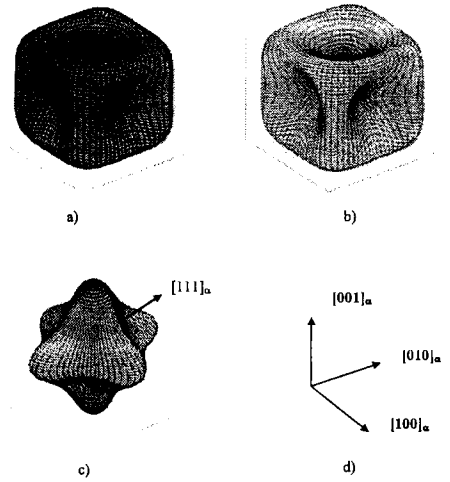

Figure 1. The parametric plot of the orientation $\{hkl\}$ dependence of elastic strain energy (under minimal thickness approximation) caused by embedding a platelet-like FCC-A1 cluster in Al-matrix oriented with respect to the Al-cubic coordinates. a) Cu; b) (postulated) Mg; and c) a CuMg3-FCC mixture. Insert d) indicates the cubic coordinates of the FCC-matrix.

Hornstra-Bartels Model

Under approximation of the minimal thickness, a platelet like cluster coherently in matrix may be treated in analogy with an epitaxial layer with substrate. The strain energy associated with the formation of the cluster can thus be calculated using Hornstra-Bartels Model [16-17]:

$$E(\xi) = \frac{1}{2} C_{ijkl} (\varepsilon_{mis}\delta_{ij} + b_i \xi_j)(\varepsilon_{mis}\delta_{mn} + b_m \xi_n) \qquad (6)$$

where b is a vector describing the positions of the epilayer lattice relative to the corresponding sites if

the epilayer and the substrate materials were identical, and $\{\delta_{ij}\}$ a Kronecker matrix. The benefit of using this model is an easy demonstration of the orientation dependence of the strain energy. The explicit formula for $\boldsymbol{b}$ vector has been derived in [16]. Fig. 1 illustrates the parametric plots of the orientation dependence of elastic strain energy for some clusters. It shows that the Cu-FCC (C_{11}=17.90, C_{12}=12.46, C_{44}=8.03) clusters has the highest strain energy when they are parallel with $\{111\}_\alpha$, and the lowest strain energy when parallel with $\{100\}_\alpha$. This agrees to the results using Eshelby's model as shown below. It explains the formation of Cu plate-like clusters on the $\{100\}_\alpha$, as experimentally observed Cu GP-zones in Al. The hypothesized Mg-FCC structure (C_{11}=4.76, C_{12}= 3.09, C_{44}=2.27) is similar to Cu. It indicates that pure Mg atoms are difficult to form plate clusters on $\{111\}_\alpha$ where they have the largest strain energy. Fig. 1 also shows the result for the FCC-A1 structure of the "quasi-disordered" mixture of Cu and Mg (1:3) that bears the lowest strain energy when parallel with $\{111\}_\alpha$. It indicates that it is the cluster mixtures of Cu-Mg, that most likely form on $\{111\}_\alpha$, that function as precursors for Ω precipitates. The high calculated pairing probability or negative SRO-parameter for Mg-Cu supports this point [18].

Eshelby's Inclusion Strain Energy

To more exactly account for the elastic strain or deformation associated with embedding of the coherent clusters in the matrix [19-24], Eshelby's elastic inclusion model can be utilized. Under an approximation of ellipsoidal shape, the elastic strain energy $E_{incl}(\xi)$ of an plate inclusion as

$$E_{incl}(\xi) = -\frac{1}{2}\sigma^*_{ij} \cdot \varepsilon^{T^*}_{ij} \qquad (2)$$

where ξ denotes the normal vector of the plate broad faces, $\{\sigma^*_{ij}\}$ the stress inside the inclusion, $\{\varepsilon^{T^*}_{ij}\}$ the eigenstrain or stress-free transformation strain of the plates that can be related to the lattice misfit $(a_p - a_m)/a_m$ with the lattice constants a_p and a_m of the non-constrained plates and the matrix. The Einstein's summation convention is used. The stress $\{\sigma^*_{ij}\}$ can be related to the constrained strain $\{\varepsilon^c_{ij}\}$ of the plates by considering the equivalency of the stress and strain of the inhomogeneous inclusion and the corresponding homogeneous inclusion:

$$\sigma_{ij}^{(I)} = C_{ijkl}(\varepsilon^c_{kl} - \varepsilon^T_{kl}) = C^*_{ijkl}(\varepsilon^c_{kl} - \varepsilon^{T^*}_{kl}) \qquad (3)$$

where $\{C_{ijkl}\}$ and $\{C^*_{ijkl}\}$ denote the elastic constants of the matrix and platelets, the $\{\varepsilon^T_{ij}\}$ the equivalent transformation strain that may be written as

$$\varepsilon^c_{ij} = S_{ijkl} \cdot \varepsilon^T_{kl} \qquad (4)$$

where the determination of the Eshelby tensor $\{S_{ijkl}\}$ for platelets of generally elliptical shape requires numerical solution of an integral equation [17-18]. When the plates are assumed to have "flat" broad faces and large aspect-ratio, an approximate formula may be employed [23]:

$$S_{ijkl} = C_{ijmn}N_{mn}(\xi)\xi_m\xi_n / D(\xi) \qquad (5)$$

with $D = \det(C_{ikjl}\xi_k\xi_l)$ and $N_{ij}(\xi)$=*cofactor* $(C_{ijkl}\xi_k\xi_l)$. Using the elastic constants and the lattice parameters from Table 1, the strain energy E_{incl} can thus be calculated for the platelets with specific orientations in the aluminum matrix. The orientation transformation of the elastic tensors can be calculated using the corresponding orthogonal matrix $\{O_{ij}\}$ as $C^*_{i'j'k'l'} = O_{ii'}O_{jj'}O_{kk'}O_{ll'}C^*_{ijkl}$. Since both matrix and the plates have cubic crystalline structures, the associated strain energy has a minimum with ξ = $\{100\}_\alpha$ and maximum with $\xi = \{111\}_\alpha$, or vice versa [25]. Therefore, only $\{100\}_\alpha$ and $\{111\}_\alpha$ platelets will be considered. For $\{111\}_\alpha$-platelets, the orthogonal matrix **O** = [1 0 $\underline{1}$; 1 $\underline{2}$ 1; 1 1 1] was used. Table 2 lists the calculated strain energy according to Eq. 2 for pure Cu, Mg (FCC-A1), Ag, Li and the quasi-disordered Cu-Mg3 cluster.

Table 2. The calculated elastic strain energy associated with the platelet-like clusters of FCC-A1 structures formed with the flat-surface normal $\{001\}_\alpha$ and $\{111\}_\alpha$ in the matrix using an Eshelby model.

Cluster	Cu	Ag	Mg	Li	Cu3Mg*
E{001} 10^{10} J/m^3	0.13	0.0051	0.056	0.0047	0.0103
E{111} 10^{10} J/m^3	0.23	0.0095	0.102	0.0070	0.0092

Discussion

The calculation of the strain energy associated with the formation of platelet-like pure metal clusters has been based on the 2nd order elastic tensor obtained using first principle total energy. It is justified by the deformation behavior of the FCC-A1 crystal structures of the elements such as Al, Cu, Mg,

Ag and Li obey Hooke's law at a small deformation scale (<0.01). However for the strain caused by relatively large misfits, the deformation has some significant deviation from linear elasticity — Hooke's law in some structures, *e.g.,* FCC-Mg in Al. Particularly for some metastable or unstable FCC structures such as Cd, Zn, Si etc., more complex description other than the linear elasticity has to be introduced to characterize the deformation behavior and to calculate the associated strain energy [18].

The result in our calculation for the Cu cluster agrees with that by Suh and Park [24] where the Asano's integral equation for Eshelby's model was used. However, the present work found the minimum of the strain energy for FCC-Mg clusters to have {100}-orientation rather than {111} [24]. The discrepancy is obviously caused by the elastic constants estimated according to the corresponding stable HCP-A3 crystal structure in [24]. The first principle calculation in this work has showed that there are substantial differences in the deformation behavior, *e.g.,* the elastic constants in Table 1, between FCC- and HCP-structures of Mg. The differences are much more significant for the other metastable or unstable FCC-A1 structures of the elements Cd, Zn and Si *etc.* [18].

Interactions between elements, such as, Cu-Mg and Mg-Si *etc.* are essential for the formation of clustering in aluminum alloys as shown in the experiments. The clusters may thus consist of more than one element, as a mixture of alloying elements. While the chemical and atomic structures of the mixture clusters are mostly unknown and difficult to ascertain, it may be effectively treated as a regular solid solution when the elastic deformation is examined. Combination of the first principle total energy calculation with a "virtual potential" construction technique [26] may offer a way to calculate the 2nd order elastic tensors for the mixture clusters. By the strain energy analysis and the element interaction analysis using thermodynamic models, it might be possible to identify potentially "useful" trace elements for forming precursors and/or "harmful" impurities that form non-precursors via 1) the short-range-order (SRO) parameter that gauges the probability for potential elements to form either clusters or SROs (atom aggregates), and 2) the orientation-dependence of the strain energy that controls the habit-plane selection of these platelet-like aggregates [18].

Acknowledgements – The authors acknowledge the financial support of the Air Force Office of Scientific Research under Grant No. S49620-01-1-0090, Dr. Craig S. Hartley, Program Monitor. BMG acknowledges support from NASA under grant NAG-1-02090.

References

1. D.L. Gilmore and E.A. Starke, Jr., Met. and Mat. Trans. A, 28A, 1399 (1997)
2. L. Reich, M. Murayama, K. Hono: Acta Mater. Vol. 46, No.17, 6053 (1998)
3. J.F. Nie, H.I. Aaronson and B.C. Muddle, in The Japan Institute of Metals Proceedings Volume 12 (JIMIC-3), Solid-Solid Phase Transformations,Part I, edited by M. Koiwa, K. Otsuka and T. Miyazaki, pp. 1128-1135 (1999)
4. C. R. Hutchinson, X. Fan, S. J. Pennycook, G.J. Shiflet: Acta Mater. 49, 2827 (2001)
5. M. Murayama and K. Hono, Scripta Mater., 44, 701 (2001)
6. J.R. Pickens, L.S. Kramer, T.J. Langan, F.H. Heubaum and F.W. Gayle, Aluminum-Lithium Alloys VI, DGM Informationsgesellchaft mbH, Garmisch-Partenkirchen, Germany, 357 (1992)
7. S. Abis, P. Mengucci and G. Riontino, Phil. Mag. A, **70**, 5, 851 (1994)
8. B M Gable, G J Shiflet, E A Starke Jr., submitted to Scripta Mater.
9. H. Suzuki, I. Araki, M. Kanno and K Itoi, Trans. Jpn. Inst. Light Met., **27**, 239 (1977)
10. D. Mitlin, V. Radmilovic, J.W. Morris, Jr., Met. and Mat. Trans. A, **31A**, 2697-2711(2000)
11. R.N. Wilson, D.M. Moore and P.J.E. Forsyth, J. Inst. Met., **95**, 177 (1967)
12. J K Lee, D M Barnett, H I Aaronson, Met. Trans. 8 A, 963 (1977)
13. G. Kresse and J. Furthmueller, *J. Comput. Mater. Sci.*, **6**, 15 (1996)
14. G. Simmons and H. Wang, Single Crystal Elastic Constants and Calculated Aggregate Properties, MIT Press (1971)
15. A F Federov, Theory of Elastic Waves in Crystals, translated by JES Bradley, Plenum Press, New York, (1968)
16. D J Bottomley and P Fons, J. Cryst. Growth, 1996, 160, 406
17. J. Hornstra and W. J. Bartels, J Crys. Growth, 44, 513 (1978)
18. A.W. Zhu, B.M. Gable, G. J. Shiflet, E A Stake Jr, work in progress
19. J D Eshelby, Progress in Solid Mechanics 2, eds. I N Sneddon, R Hill, North-Holland, Amsterdam, 1961, p89-140
20. R J Asaro and D M Barnett, J. Mech. Phys. Solids 23, 77 (1975)
21. S C Lin and T Mura, Phys. Stat. Sol. (a), 15, 281 (1973)
22. A. W. Zhu and E. A. Starke Jr, Acta mater. 49, 3063 (2001)
23. Takehiko Eto, A Sato and Mori, Acta Metall., 26, 499 (1978)
24. I. S. Suh and J K Park, Scripta Metall. Mater. 33, 205 (1995)
25. D.B. Laks, L.G. Ferreira, S. Froyen and A Zunger, Phys. Rev. B, 46, 12587 (992)
26. C. S. Hartley, Acta Mater., 51,1373 (2003)

FORMATION OF CLUSTERS FOR PRECIPITATION IN AL-CU-MG-(AG, SI) ALLOYS: SHORT-RANGE-ORDERING AND STRAIN-ENERGY ANALYSIS

Aiwu Zhu, Brian M Gable, Gary J Shiflet, Edgar A Starke Jr.

Department of Materials Science and Engineering,

University of Virginia, Charlottesville, VA 22904-4745, USA

ABSTRACT

In order to produce a fine and uniform dispersion of the selected strengthening precipitates for optimized mechanical properties of Al-Cu-Mg-X alloys, the nucleation rate of the favored precipitates must be augmented. One strategy to accomplish this is to enhance the formation of their precursors through trace elemental additions such as Ag, and/or the elimination of harmful impurities, *e.g., Si.* Based on the CALPHAD databases, this work analyzes the short-range-ordering related to the addition of *Ag, Si* and other potential trace elements to the Al-Cu-Mg system. To anticipate the orientation selection of the plate-like clusters formed through short-range-ordering of trace additions, the anisotropy of the associated strain energy was considered using the 2nd order elastic tensors calculated from the first principle total energy approach.

INTRODUCTION

Al-Cu-Mg-X alloys were the earliest developed and most advanced age-hardenable light metal systems. There has been a continuous effort to improve this system for aerospace structural applications [1]. Since the precipitation hardening provides the majority of strength of the alloys, it is the strength of 2nd phase precipitates and precipitate structures that essentially control the yield strength, creep resistance and fracture toughness. For mostly plate-like precipitates, dislocation slip simulations [2] have shown that a fine and uniform dispersion of precipitates having different habit planes, *e. g.*, $\{111\}_\alpha$ Ω and $\{100\}_\alpha$ θ″/θ′ in Al-Cu-Mg (with high Cu:Mg ratio), is desired for optimum mechanical properties. This paper describes our recent work on precipitation of the $\{111\}_\alpha$ Ω phase. The emphasis of this paper is on thermodynamic analysis of the effect of trace element (Ag, Si etc.) additions on nucleation of the Ω phase in the Al-Cu-Mg alloys.

STABLE PHASES AND PHASE EQULIBRIA

Experimental investigation of Al-Cu-Mg in the Al-rich corners with Cu:Mg ratio >1 shows that the stable 2nd phases that may exist within Al FCC solutions are θ (Al_2Cu), S (Al_2CuMg) and T ($Al_{32}(CuMg)_{49}$) [3]. Details of the phase equilibria can be calculated based on CALPHAD models [4-6] as illustrated in Fig. 1a. Accordingly, one may carefully choose alloy compositions to achieve desired 2nd phase(s), and avoid undesired one(s).

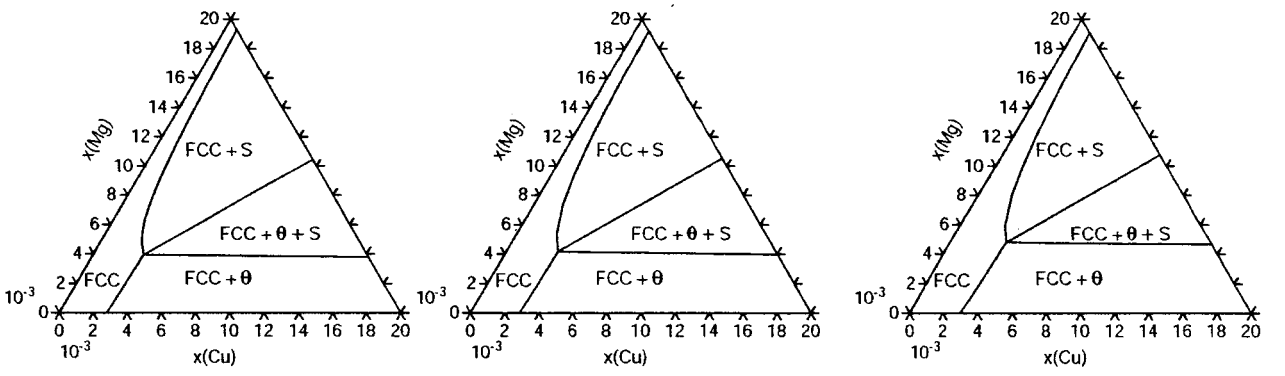

Al-Cu-Mg, 600 K **Al-Cu-Mg-0.005Si, 600K** **Al-Cu-Mg-0.01Ag, 600K**

Figure 1. Calculated isothermal sections for Al-Cu-Mg, Al-Cu-Mg-0.005Si, Al-Cu-Mg-0.01Ag at the Al-rich corner at 600 K.

META-STABLE PHASES

Stable equilibrium phases as shown in the phase diagrams may be obtained through aging treatment for long time and at high temperatures. However for most age-hardenable aluminum alloys it is the metastable 2nd phases that more effectively strengthen the materials. Metastable 2nd phase particles, structurally coherent or semi-coherent with the Al matrix, are formed prior to the stable phases since they have lower interfacial energies and hence a lower energy barrier for nucleation. These phases often have fine (small in size, and *e.g.* large aspect ratio for plate or rod-like precipitates) and uniform distributions. Although metastable, they normally can be maintained at lower service temperatures. The Ω and θ′ in the recently developed Al-Cu-Mg-Ag-X alloy system are examples. Both Ω and θ′ have the same chemical composition as the θ phase (Al_2Cu). θ′ has a tetragonal crystal structure and the plate-like particles are formed with habit planes $\{100\}_\alpha$. The broad faces of the platelets with normal direction $[001]_{\theta'}$ are coherent with Al-matrix. The precipitates are relatively stable below 150°C depending on compositions and deformation states although they are eventually replaced by θfor a long time at high temperatures. Several crystal structures have been proposed for the Ω phase. Auld suggested a monoclinic structure [7]. A widely accepted structure [8-10] is orthorhombic with space group (Fmmm). Based on analysis of the convergent-beam electron diffraction (CBED) patterns, Garg and Howe [11] advocated a tetragonal structure (I4/mcm) that is only a metastable $\{111\}_\alpha$ variant of the equilibrium θ phase. The results of first principle calculations have ruled out the monoclinic structure due to its positive enthalpy of formation [12]. The energetic difference between the tetragonal structure and the orthorhombic one is negligible as shown below. The Ω phase precipitates as a uniform dispersion of thin hexagonal platelets with $\{111\}_\alpha$ habit planes.

The broad faces with normal direction $[001]_\Omega$ are coherent with the Al matrix. Although they may eventually be replaced by the θ phase, which has a $\{100\}_\alpha$ habit plane, after *e. g.* 100 days at 523 K [13], the Ω phase can be retained after 72 h at 623 K [7] or 132 days at 473 K [14] when trace additions of Ag are present. Z-contrast HRTEM and TEM-EDS studies have showed that the enhanced thermal stability of the Ω phase precipitates can be attributed to either Mg and/or Ag atoms that segregate onto the broad interfaces [15].

PRODUCTION OF DESIRED PRECIPITATES

For Al-Cu-Mg alloys having composition in the (FCC+θ) and (FCC+θ +S) phase fields, an aging treatment may produce stable phases such as θ and S, and metastable phases such as θ', Ω and σ ($Al_5Cu_6Mg_2$) depending on aging conditions (temperature and time), alloy compositions and pre-age treatment (solution treatment, quenching and deformation [16]). It is evident that the nucleation processes are crucial for the production of the metastable phases especially for age-hardenable aluminum alloys. While appropriate compositions and relatively low temperature aging insure that the driving forces are high enough for the metastable phases (usually possessing lower interfacial energies than the corresponding stable phases), it is mostly the density of the pre-existing inhomogeneities serving as nucleation sites that controls the nucleation rates and hence the precipitate structures in the solid solutions. These inhomogeneities can be dislocations introduced through pre-age deformation (T8 treatment) and/or the atom aggregates or other phases that acts as precursors. Generally for the atom aggregates or other metastable particles there are two mechanisms for transformation to the more thermodynamically stable precipitates. Local strain fields around the clusters due to the lattice misfits provide accommodation for the local strain associated with nucleation of the more stable precipitates that themselves possess a lattice misfit. Since the strain field of platelet-like clusters is highly orientation dependent, it has a significant effect on the habit planes of the precipitates. Examples are Mg-rich clusters for the T_1 $\{111\}_\alpha$ in Al-Li-Cu-Mg and Ω $\{111\}_\alpha$ phase in Al-Cu-Mg-(Ag). In addition, the Cu $\{100\}_\alpha$ clusters or [G.P.] zones often evolve into the metastable and equilibrium precipitates, *e.g.*, the θ' or θ $\{100\}_\alpha$ plates in Al-Cu based alloys.

X-ray diffusse scattering studies of the early stages of aging in Al-Cu-Mg alloys indicated that GP zones comprised of Cu and /or Mg can be associated with short-range-ordering on or along $\{100\}_\alpha$ planes [17]. The θ'/θ''-precipitates evolve from Cu GP zones or clusters. The Cu GP zones form as thin platelets on $\{100\}_\alpha$-planes from supersaturated solid solutions (SSSS) [18]. Atom probe field ion microscopy (AP-FIM) used in conjunction with analytical TEM has revealed the existence of individual Cu and Mg clusters and Cu-Mg clusters in an Al-0.017Cu-0.003Mg (atomic fraction) alloy [19]. Although trace additions of Mg have been proven to be crucial, there has been no direct evidence showing the effects of these clusters on the nucleation and formation of Ω precipitates. The precipitation of the S phase obviously reduces the chemical potential of Mg in the Al-SSSS and hence is deleterious to Ω precipitation.

The addition of Ag not only enhances the coarsening resistance of Ω plates but also plays a role in the formation of Ω precipitates on $\{111\}_\alpha$. AP-FIM and TEM studies discovered individual Cu, Mg and Ag clusters in quenched specimens of Al-Cu-Mg-Ag alloys [19]. Additionally, Mg-Ag co-clusters were found immediately after commencement of aging [19-21]. Three dimensional atom probe (3D-AP) analysis of an Al-0.019Cu-0.003Mg-0.002Ag alloy revealed more details about the morphology and orientation of these clusters [22-23]. The Mg-Ag clusters, which were formed at the earliest stage of aging, did not have a well-defined shape. Some Mg-Ag-Cu co-clusters were later found to form with a thin platelet like shape on $\{111\}_\alpha$.

These $\{111\}_\alpha$ platelet clusters, or GP zones, finally evolved into well-defined Ω particles. It is evident that the addition of Ag, greatly enhanced the nucleation of Ω precipitates in Al-Cu-Mg-Ag, as compared with Al-Cu-Mg. This enhancement can be attributed to the Mg-Ag co-clustering and to the formation of {111} Cu-Mg-Ag plate-like co-clusters (or GP zones).

Silicon additions have long been used to increase the strength and hardness of Al-Cu-Mg alloys (arising from enhanced precipitation of strengthening 2nd phases). The effect of a silicon addition on Ω precipitation has been systematically studied using a series of Al-Cu-Mg-Si alloys [24]. It was found that a Si addition quelled the formation of Ω but enhanced the precipitation of the competing phases θ′, S and σ. There was no direct observation of cluster formation in the alloys.

CALPHAD MODELS FOR AL-CU-MG-(AG, SI) ALLOYS

The thermodynamic models for Al-Cu-Mg-(Ag, Si) are available in the CALPHAD databases [5-6] and some have been published in the literature [4]. The interaction parameters for Gibbs energies of each phase in the models are obtained through optimization according to the related solid-solid or solid-liquid phase eqilibria that have been experimentally measured. The stable phases concerned here are FCC-A1, S and θ as shown in Fig. 1a. As a metastable phase, Ω, possessing the same chemistry and similar crystalline structure to θ, has not been modeled. In order to compare Ω with θ energetically, first principle total energy calculation was performed using the Vienna *ab initio* simulation program (VASP) [25] together with the optimized pseudo-potentials supplied with the software package. The LDA (Local-Density Approximation) was used for electronic exchange correlation potentials. The GGA (generalized gradient approximation) did not produce any significant changes in the results. The basis-set cut-offs were set to "high accuracy" and k-point meshes were set using "Monkhorst-Pack" or Γ-centered settings. As shown in Table 1, both the tetragonal and the orthorhombic structures of the Ω phase have formation enthalpies that are essentially the same as that of the θ phase. According to the TT-Al data [6] and COST2 database [5] that were compiled via the CALPHAD method, the formation enthalpy of the equilibrium θ phase is -164 meV/atom. Although the entropy related term of Ω phase is not known, it may thermodynamically be treated as equivalent to the θ phase. Solubility of Ag [26] in Ω is negligible and there is no report on Si solubility. The Ω can be treated as a two-sublattice ordered compound, similar to that of θ in the databases. Modifying the parameters of θ according to these calculated formation enthalpies (-0.169 eV/atom) of the Ω phase yields little difference in the phase equilibria as shown in Fig. 1.

Therefore, sin orderto analyze Al-Cu-Mg-(Ag-Si) systems at the Al-rich corner containing FCC-A1, S and Ω (as θ-phase is suspended), the thermodynamic equivalence of Ω with θ allows the use of the available interaction parameters for each phase that has been optimized based on its phase equilibria. Calculated phase diagrams of Al-Cu-Mg, Al-Cu-Mg-0.005Si and Al-Cu-Mg-0.01Ag at 600 K are given in Fig. 1. This figure shows that the addition of Si has little impact on the phase equlibria while a Ag addition shifts the boundary between the (FCC+Ω) phase field and the (FCC+ Ω +S) phase field to higher Mg concentrations.

Table 1. VASP Calculated Formation Enthalpies of Proposed Crystal Structures for Ω and θ phases as compared with that of θ obtained from optimization using thermodynamic models.

	Proposed structure Lattice Parameters	ΔH, eV/atom
θ	Tetragonal (I4/mcm): 6.063, 4.87	-0.168
Knowles' Ω	Orthorhombic(Fmmm):4.96,8.59,8.46	-0.167
Garg & Howe's Ω or θ_m	Tetragonal (I4/mcm): 6.066,4.96	-0.169
θ as modeled in COST507 etc.	2 sub-lattice ordered compound with composition Al2-Cu	-0.164

The enhancing effect of a Ag addition on the formation of Ω precipitates can be related to the shift of the phase boundaries. Strong attractive interaction between Ag and Mg (as shown below) lower the chemical potential of Mg in the Al solid solution and hence lowers the driving forces for S-phase nucleation. Accordingly the formation of Ω (equivalent with θ) is enhanced at the expense of the S-phase.

CLUSTERING IN SOLID SOLUTIONS OF AL-CU-MG-(AG, SI)

The Al-Cu-Mg-(Ag, Si) (FCC) solid solution was modeled as a sub-regular solution using a Redlich-Kirst-Muggianu's formula [27]. The atomic interactions in the solutions could be complex but was assumed to be reflected in the thermodynamic functions of the solutions. As the first approximation, only the 1st neighbor interaction between atoms was considered. Using a quasi-chemical model for high-order systems [28], the pairing probabilities ζ_{ij} between different elemental atom *i* and *j* was calculated using

$$\frac{\zeta_{ij}^{\ 2}}{(x_i - \sum_{p=i,q} \zeta_{pq}) \cdot (x_j - \sum_{p,q=j} \zeta_{pq})} = \exp\left(-\frac{2\Omega_{ij}}{kT}\right) \qquad (2)$$

where x_i is the i atomic fraction, k the Boltzmann constant and T the temperature. The pair interaction (bonding) energy Ω_{ij} between unlike atoms *i* and *j* with respect to those of the like-atom interactions was obtained as $\Omega_{ij} = \Delta H_{mix.}(i, j) / z\, x_i\, x_j$ where z is the coordination number of the nearest neighbors in the FCC structure (=12). $\Delta H_{mix.}(i, j)$ the heat of mixing between the two elements, was retrieved from the thermodynamic models mentioned above. Solving Eqs. (2), the Warren-Cowley ordering parameters $SRO(i, j) = 1 - \zeta_{ij}/x_i x_j$ was obtained. The W-C SRO parameter indicates the tendency for short-range-ordering or co-clusters between different elemental atoms. A negative $SRO(i, j)$ refers to an attractive interaction and co-clustering between *i* and *j*, while a positive one to a repulsive interaction between the atoms in the solution.

Fig. 2 illustrates the Warren-Cowley parameters calculated using Eq. (2) for elemental atomic pairs in Al-0.0175Cu-xMg, Al-0.0175Cu-xMg-0.01Ag and Al-0.0175Cu-xMg-0.005Si solid solutions at 600 K (x=0.005 to 0.06). The most negative SRO (Cu-Mg) indicates the most dominating tendency of Cu-Mg co-clustering in Al-0.0175Cu-xMg. Addition of 0.005Si and

0.01Ag decreases the tendency of Cu-Mg co-clustering (Fig. 2(a)). Dominating co-clustering will occur between Cu-Si, Mg-Si in Al-0.0175Cu-xMg-0.005Si (Fig. 2(b)) and overwhelmingly between Mg-Ag in Al-0.0175Cu-xMg-0.01Ag. These calculations clearly agree with the AP-FIM and TEM observations in the Al-Cu-Mg alloy, and AP-FIM, TEM and 3D-AP observations in the Al-Cu-Mg-Ag alloy, mentioned previously. Regarding the alloys containing Si, although there is no direct observation of the cluster formation, the deleterious effect of a Si-addition on Ω precipitation [24] can be attributed to the decrease in Cu-Mg clusters that is necessary for the Ω formation and the strong tendency of Mg-Si co-clustering that consumes Mg from the solution.

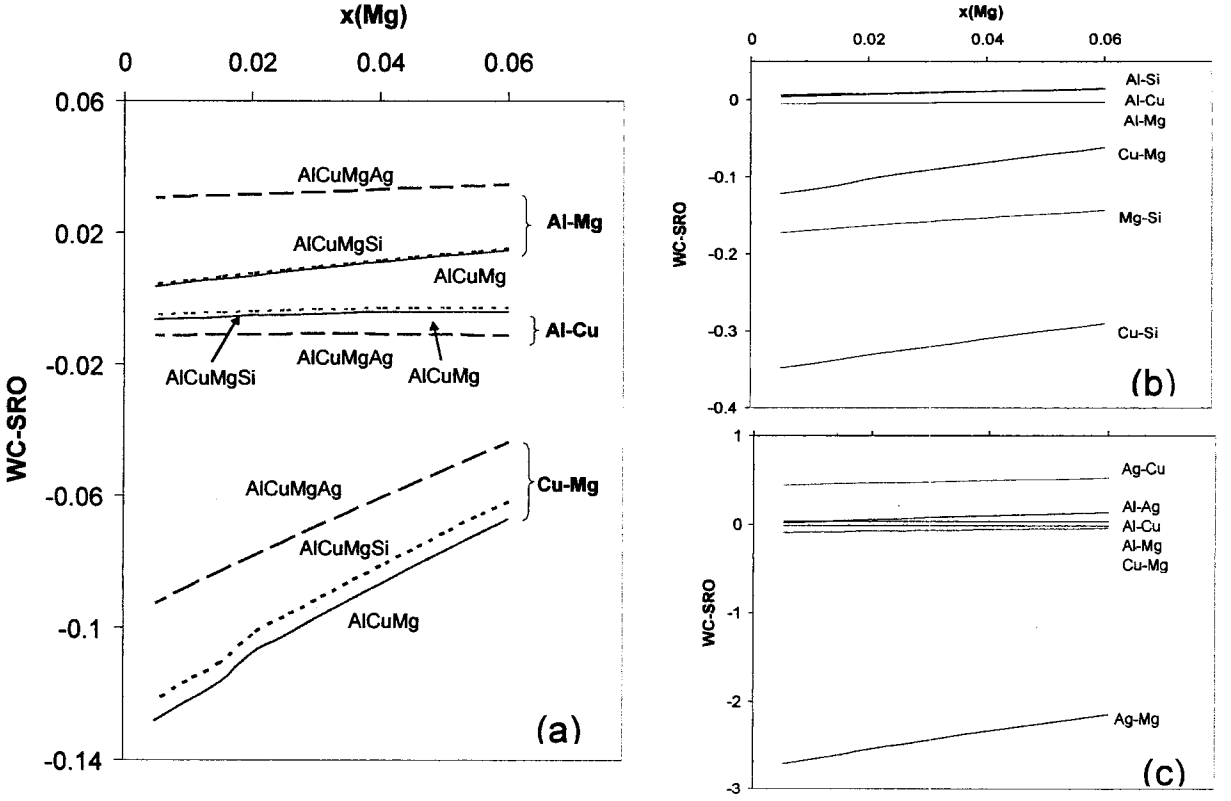

Fig. 2 Warren-Cowley SRO parameters for each pairs of elements in Al-0.0175Cu-xMg, Al-0.0175Cu-0.01Ag and Al-0.0175Cu-0.005Si solid solutions at 600 K.
(a). Comparison of the SRO(Al-Mg), SRO(Al-Cu) and SRO(Cu-Mg) in the three alloys
(b). SRO parameters of each pair in Al-0.0175Cu-xMg-0.005Si
(c). SRO parameters of each pair in Al-0.0175Cu-x-Mg-0.01Ag

The extremely strong interaction between Ag-Mg [4] used here in Al-Cu-Mg-Ag, although qualitatively agreeing with experimental observations, may need to be assessed more carefully in order to integrate the model more consistently into the Al-Cu-Mg-Ag-Si system that is under study.

STRAIN ENERGY ANALYSIS

As discussed above, the plate-like precipitates select the habit planes in the SSSS during their nucleation stage. The habit plane selection of the precipitates depends on the local strain orientation of the precursors or clusters since subsequent precipitate nucleation must accomodate their own lattice misfit strain. However, the orientation of most platelet-like clusters, is controlled by the anisotropy of their lattice-misfit induced strain. The strain energy analysis of those clusters in Al solid solutions may provide the information as to which clusters or co-clusters will assist in the formation of the desired precipitates having specific habit planes.

The strain energy analysis of the pure elemental clusters, using 2nd order elastic constants calculated based on the first principle total energy has been reported [29]. The epitaxial layer model by Hornstra and Bartels [30] and the elastic inclusion model by Eshelby [31] were employed for the calculations. The results show that the Cu-FCC platelet clusters have the highest strain energy when they are parallel with $\{111\}_\alpha$, and the lowest strain energy when parallel with $\{100\}_\alpha$. This explains the formation of Cu plate-like clusters on the $\{100\}_\alpha$, as experimentally observed Cu GP-zones in Al. The hypothesized FCC structure of Mg is similar to Cu but with a lower anisotropy. A hypothesized stable CuPt (L1)-structure of Mg-Ag co-cluster also shows the similar lower anisotropy as compared with a Cu cluster. A preliminary calculation of the "FCC" structure of the "quasi-disordered" mixture of Cu and Mg (with ratio1:3) has the lowest strain energy when the co-cluster platelet is parallel with $\{111\}_\alpha$. This indicates that both pure Mg atom clusters and MgAg co-clusters are difficult to form plate clusters on $\{111\}_\alpha$ where they would have the largest strain energy. The addition of Cu atoms in the Mg clusters may allow the Mg-rich Mg-Cu cluster to select $\{111\}_\alpha$ habit planes. Details studies will be reported elsewhere. Combining with the above SRO analysis, these results indicate that pure Mg clusters are not the precursors for Ω precipitates as claimed in the discussion part of [19] and in the calculation [32]. Instead it is the clusters of Cu-Mg, that most likely form on $\{111\}_\alpha$, that may function as precursors for Ω precipitates in Al-Cu-Mg. For Al-Cu-Mg-Ag alloys, Mg-Ag clusters may not directly act as precursors but instead Mg-Ag-Cu co-clusters that form on $\{111\}_\alpha$ may act as precursors as observed in 3D-AP [22-23]. However, an exact strain analysis of co-clusters of Mg-Ag-Cu using first principle calculation is formidable.

These results of our study related to Mg and Mg-Ag clusters is not in agreement with those obtained by Suh and Park [32] who employed Eshelby's elastic inclusion model implemented by Asano's integral equation [33]. The discrepancies are obviously caused by the elastic constants estimated according to the corresponding stable HCP-A3 crystal structure in [33]. First principle calculations have shown that there are substantial differences in the deformation behavior, *e.g.*, the elastic constants in Table 1, between FCC- and HCP-structures of Mg.

Regarding clusters in Al-Cu-Mg-Si, the instability of most of these "FCC" structures prevents using the models based on 2nd order elastic constant calculations based on the first principle total energy.

CONCLUSION

Thermodynamic analysis of clustering based on the CALPHAD approach and the strain energy analysis of the clusters provide potential tools to identify elements that are helpful or deleterious in enhancing the formation of the desired precipitates in age hardenable Al-Cu-Mg alloys.

Acknowledgement – the authors are indebted to the financial support of support of the Air Force Office of Scientific Research under Grant No. S49620-01-1-0090, Dr. Craig S. Hartley, Program Monitor. BMG acknowledges support from NASA under grant NAG-1-02090.

References:

[1] E.A.Starke Jr., J.T. Staley, Prog. Aerospace Sci. 1996, 32, 132
[2] A.W. Zhu, A. Csontos and E.A. Starke, Jr., Acta mater., 1999, 47, 1713.
[3] G.B. Brook, Precipitation in Metals, Special Report No. 3, Fulmer Research Institute: UK, 1963
[4] M.S. Lim, J.E. Tibballs and P.L. Rossiter, Z. Metallkd., 1997, 88, 2, 162.
[5] COST507 'Database for Light Alloy Design' , EU COST507 project, Round II, 1998
[6] ThermoTech Ltd., TT Al-based Alloys, 1999.
[7] J.H. Auld, B E Williams, *Acta Cryst.*, 1966, **21**, 830
[8] S. Kerry and V.D. Scott, Metals Sci., 1984, 18, 289..
[9] K.M. Knowles and W.M. Stobbs, Acta Cryst., 1988, B44, 207.
[10] B.C. Muddle and I.J. Polmear, Acta Metall., 1989, 37, 777.
[11] A. Garg and J.M. Howe, Acta Metall., 1991, 39, 1939.
[12] A.W.Zhu, B.M. Gable, G.J. Shiflet, E.A. Starke Jr, Adv. Eng. Mater. 4, 11, 839-845, 2002
[13] S.P. Ringer, B.C. Muddle, I.J. Polmear, in The ICAA-3 vol2, ed. Arnberg L, Lohne O, Norwegian Institute of Technology, Trondheim, Norway, 1992, 187
[14] R.J. Chester, I.J. Polmear, Micron 11, 1980, 311
[15] C.R. Hutchinson, X. Fan, S.J. Pennycook and G.J. Shiflet, Acta Metall. 2001, 49, 2827
[16] N. Unlu, B.M. Gable, G.J. Shiflet and E.A. Starke, Jr. Materials Science Forum 2002; 396-402:801.
[17] Yu.A. Bargarytski, Doklady, Akad. Nauk SSSR, 87, 559 (1952)
[18] E. Hornbogen, Aluminum 1967, 43,115
[19] S.P. Ringer, K, Hono, I.J. Polmear and T. Sakurai, Acta mater. 1996, 44, 1883
[20] K. Hono, T. Sakurai, I.J. Polmear, Scripta Metall. Mater. 1994, 30, 695
[21] S.P. Ringer, T. Sakurai and I.J. Polmear, Acta mater. 1997, 45, 3731
[22] M. Murayama and K. Hono, Scripta Mater. 1998, 38, 1315
[23] L. Reich, M. Murayama and K. Hono, Acta. Mater., 1998, 46, 17, 6053
[24] B. M Gable, GJ Shiflet, EA Starke Jr, The effect of Si addition on the precipitation of W in Al-Cu-Mg-(Ag) alloys, accepted by Scripta Mater.
[25] G. Kresse and J. Furthmueller, *J. Comput. Mater. Sci.*, 1996, **6**, 15
[26] N. Sano, K. Hono, T. Sakurai and K. Hirano, Scripta Metall. Mater. 1991, 25, 491
[27] N. Saunders and A.P. Miodownik, CALPHAD-Calculation of Phase Diagrams, Pergamon Materislas series v. 1, 1998
[28] A.W. Zhu and G.J. Shiflet, submitted to Bulk Metallic Glasses, TMS 2004, Charlotte USA
[29] A.W. Zhu, B.M. Gable, G.J. Shiflet and Starke Jr EA, submitted to ASM 2003, Pittsburgh, USA
[30] J. Hornstra and W. J. Bartels, J Crys. Growth, 44, 513 (1978)
[31] J D Eshelby, Progress in Solid Mechanics 2, eds. I N Sneddon, R Hill, North-Holland, Amsterdam, 1961, p89-140
[32] I. S. Suh and J K Park, Scripta Metall. Mater. 33, 205 (1995)
[33] R J Asaro and D M Barnett, J. Mech. Phys. Solids 23, 77 (1975)